Met O (APR) Turbulence and Diffusion Note No. 236

Determining cross-wind variance for low-frequency wind meander

by

R.H. Maryon

January 1997

Met O (APR) (Atmospheric Processes Research)
Meteorological Office
London Road
Bracknell
Berkshire, RG12 2SZ

Note:

DETERMINING CROSS-WIND VARIANCE FOR LOW-FREQUENCY WIND MEANDER

R.H.Maryon

January 1997

Introduction. The diffusion parametrization for the NAME dispersion model is described in Physick & Maryon (1995) and Ryall & Maryon (1996). It became evident from comparisons with other models (Maryon et al 1996) and the ETEX evaluations that NAME 2 was tending to overpredict air concentrations. An important reason for this was the absence of horizontal wind meander---in NAME 1 the diffusion coefficient was designed to cover all horizontal fluctuation. Lateral dispersion for longer time periods (up to 12hr) was studied by Moore (1974, 1976), and the application to the ADMS model reviewed in Davies & Thomson (1995). It was decided to utilize the MRU (Cardington) surface wind data for the three years 1988 - 1990 to determine a horizontal velocity variance for meander, which could be used in a Moore-type formula. Details of the measurement technique and quality control of the time series of 10 minute means are given in Davies & Thomson. In contrast to, and as a supplement to, these authors, it was decided to use spectral techniques rather than piecewise analyses of the data.

Nature of the problem. The existing turbulence parametrization for the NAME model is based upon empirical formulae which were mostly obtained over relatively short time periods. The mesoscale, limited area and global models are resolved at about 16, 49 and 90km respectively, whereas the wind fields are available at intervals of 1, 3 and 6 hr---the temporal resolution is coarse compared with the spatial. The situation is entirely different from that of CFD or LES, where the timescales of the resolved eddies are large compared to the timestep. It is not a straightforward matter to define the frequencies of oscillation required to fill the 'spectral gap' between the high-frequency turbulence and the resolved motions. The greater constraint on the NAME parametrization is the time resolution of the input wind fields, ΔT_F, say. This can represent an oscillation of period $2\Delta T_F$ only, ranging from 2 hr for the mesoscale to 12 hr for the global grids. Addressing the problem of the temporal gap could presumably account for all the missing fluctuation, although there would no doubt be some ill-defined overlap with the somewhat better resolved spatial fields.

The Spectral Analysis of long-period time series of wind measurements. The general strategy to be adopted requires careful consideration. One way forward is to use the techniques of spectral analysis to obtain the velocity variance over a required band of frequencies. The oscillations between $2\Delta T_F$ and the frequency regarded as covered by the turbulence statistics constitute the meander variance, $\sigma^2_{v,\ell}$. This represents motions resolved perpendicularly to the mean wind. If the Cardington 10-minute means are processed a month at a time a first reaction is to compute a monthly mean and rotate the observed u and v components using the direction of the monthly mean vector as the x axis. The resolved v's might be

used for the spectral analysis. Clearly this would not produce a realistic figure for $\sigma_{v,\ell}$, because there will be spells of wind of widely differing direction. To illustrate this trivially, consider a monthly mean aligned along 270deg. Assume there is also a significant period in which the wind approximated 180deg. *The shorter-term 'mean' wind at 180deg will register as a cross-wind fluctuation on the 270deg axis. And so will the along-wind turbulence*. If the mean wind is representing a slow oscillation, it may not matter too much if we are interested in higher frequencies. It is clear, however, that spectrally, $\sigma_{v,\ell}$ will be greatly contaminated by fluctuations proper to $\sigma_{u,\ell}$ (and possibly with some residuals from the mean 180deg wind). There may also be situations where the monthly mean wind vector is close to zero, due to mutual cancellations.

The unavoidable question is raised: What is the mean wind? The answer depends upon the problem. If we are interested in fluctuation below $2\Delta T_F$, then the mean wind should be measured over a period not greatly exceeding that interval, so as to minimize problems analogous to those just described. For a spectral analysis, then, a practicable procedure might be to compute a moving average of the data of length about $2\Delta T_F$, from which the mean wind vector at any instant (or more specifically, that for an individual 10-minute period) can be determined. Then the $u(t), v(t)$, series can be resolved against x, y axes defined by that vector at time t. Using the monthly mean, of course, is the limiting 'moving average', equal in size to the data length.

Such a technique would by no means be problem free. Suppose there is a steady wind at 230deg which swings almost instantaneously to 310deg on a frontal passage at time t_f, and continues steady. A moving average of length N will register 230deg until it is within $N/2$ of t_f, when it will start to veer---and be in error. The error will gradually increase until, at t_f it will momentarily correct itself. Afterwards the moving average will be in error in the opposite sense, decreasing until the mean is correct again at time $t_f + N/2$. The error is of the shape shown diagramatically in Figure 1. In spectral terms, the varying mean wind alone will produce both long period fluctuations in error (effectively removable if attention is confined to the high frequency parts of the spectrum) and short (which will contaminate).

Now consider a steady 230deg wind which at some point veers steadily over a period N to 310deg (Figure 2). Similar considerations show that the moving average will generate (removable) error forming a uniform oscillation of period $2N$. Figures 1 and 2 are limiting cases of a uniform rate of change of the wind vector through the given angle. For wind oscillations following a perfect sine wave, the 'error' associated with a long filter will follow a perfect sine wave of the same frequency (Figure 3), BUT, if the wind oscillatons are of period $2\Delta T_F$ or less, the oscillations will of course constitute the meander, not the mean wind.

For irregular changes in direction we are likely to find a combination of high and low frequency error components from which the higher frequency bands will

contaminate the results of the spectral analysis, and the above arguments imply that contamination may be generated by either turbulent or local mean components. It can only be claimed that a filter of length approximating $2\Delta T_F$ should minimize the error. Filters of period less than $2\Delta T_F$ would remove meander.

The spectral analysis: method. A spectral analysis was carried out on the Cardington data set of 10-minute winds observed quasi-continuously during the period 1988-1990. There were large gaps, but 27 individual months were deemed suitable for analysis. For these cases the power extending from the high frequency end of the spectrum to the frequency $f = 1/(2\Delta T_F)$ was computed. The Nyquist frequency $f_N = 1/(2\Delta t)$, where Δt is the interval between successive values of the time series, i.e. f_N corresponds to a period of 20min.

The package used was the NAG FORTRAN Library Mark 13 routine G13CAF. This computes the smoothed sample spectrum

$$\hat{f}(\omega) = \frac{1}{2\pi}\left(C_0 + 2\sum_{k=1}^{M-1} w_k C_k \cos(\omega k)\right) \qquad (1)$$

by finite Fourier Transform for frequencies

$$\omega_i = \frac{2\pi i}{L}, \qquad i = 0,1,2\ldots\frac{L}{2},$$

where L (taken as 200) is the frequency division of the spectrum, C_k is the covariance at lag k, and M (taken as 100) the cutoff of the lag window (i.e. of the covariance function). The Parzen smoothing window was utilized; this is defined

$$w_k = 1 - 6\left(\frac{k}{M}\right)^2 + 6\left(\frac{k}{M}\right)^3 \qquad 0 \le \frac{k}{M} \le 1/2,$$

$$w_k = 2\left(1 - \frac{k}{M}\right)^3 \qquad 1/2 \le \frac{k}{M} \le 1.$$

The Parzen window was found to be trouble-free in comparison with the other options, including rectangular, which occasionally caused the package to crash by generating negative lobes.

Expression (1) is a two-sided form, yielding half the variance appropriate to each ordinate $\left(\hat{f}_i \times \frac{2\pi}{L}\right)$; thus the total variance is from

$$\sigma^2 = \frac{4\pi}{L}\left\{\frac{\hat{f}_0}{2} + \Sigma_i \hat{f}_i\right\},$$

with obvious adaptations for subsections of the spectrum. This expression was confirmed by comparison with conventional calculations of variance. Table 1 lists the period (or 'wavelength') $\lambda = L/i$ = 1/f for $L = 200$, in terms of cycles and (for 10-minute meaned data) hours. In view of the smoothing inherent in the spectral technique, the periods 11.1, 6.67 and 2.08hr were deemed appropriate to use for $2\Delta T_F = 12, 6$ and 2 hr, i.e. for the global, limited area and mesoscale grids respectively.

i	λ	Period (hr)
0	∞	∞
1	200	33.33
3	66.67	11.1
5	40	6.67
10	20	3.33
16	12.5	2.08
33	6.06	1.01
100=L/2	2	0.33

Table 1. Sample ordinates for a spectrum frequency division L = 200 and 10-minute meaned data.

In full the numerical procedure was to:

1. Read one month's Cardington sonic anemometer data.
2. Process the data to extract 10-minute means.
3. Rotate the u, v values from (varying) sonic axes to a fixed axis.
4. Compute 12, 6 and 2 hr moving averages of the u, v series by applying moving averages of 73, 37 and 13 values (i.e. including an additional 10 minute mean for symmetry; the extremities of the time-average sequences were filled with a small non-zero value).
5. Rotate the u, v series again so that the running mean wind vector becomes the x-axis for each 10-minute value.
6. Use the v-components so obtained for the spectral analyses.

Sample spectra, for November 1988, are illustrated in Figure 4: note the impact of determining the v-component using 12, 6 and 2 hr running means. The slope at the high frequency (unprocessed) end in (a) and (b) approximates 1.7, so is not far from the -5/3 of inertial subrange and reverse energy cascade theory.

A problem was posed by one or two truncated series, and by occasional gaps in the data, in even the 27 months with the most complete records. Tests showed that omissions of a block of a few hundred from an otherwise complete series of around 4000 could make a difference of a few percent in the result of the spectral analysis, the only systematic effect being the loss of power at low frequencies if the series length were significantly shortened. The loss of low-frequency power was of no great significance to the project, and a decision was made to ignore (close up) the occasional gap and truncation, and utilize as many of the long observational records as possible. The effect of a gap, after all, is only to alter a sequence of *synoptic realizations*, here and there, in ways which need not be unduly inconsistent with real weather transitions, and although transients would no doubt result, the effect on the spectra from very long time series should be small. In any event, the acceptance of these small perturbations was considered preferable to discarding long lengths of potentially useful data.

The spectral analysis: results. The spectral density was integrated between the high frequency limit, f_N, which, in view of the low power at high frequencies, was regarded as an acceptable limit for the turbulence parametrizations, and a number of frequencies $f = 1/2\Delta T_F$ applicable to the different grids--- i.e. $\Sigma = \int_{f_N}^{f} \hat{f} d\omega$.

Scrutiny of the results suggested that 13 October-March cases fell into a typical winter pattern (although naturally there is considerable scatter) and 8 May-August cases into a summer pattern, although in formal statistical terms there was no significant difference between the summer and winter variances (some differences do appear later, see below). No doubt with a really large sample a seasonal cycle would be apparent. Tables 2.1 to 2.3 list the mean statistics for the summer and winter cases and some additional analyses for April and September. Table 3 contains a summary of the overall means, which were computed by giving equal weighting to the winter and summer means. For the April and September months the means approximated more to the summer values but with variation more typical of the winter; in addition, two of the April series were significantly truncated. The means for the April and September cases (Table 2.3) were comparable, it will be noted, with Table 3.

A parametrization for meander would also require suitable timescales, and this again raises the question of the relative resolutions of grids with a given grid-length for which winds are available only at relatively long intervals ΔT_F. Clearly the ensemble timescale for meander, $\tau_{v,\ell} < 2\Delta T_F$, and it seems reasonable to take $\tau_{v,\ell} \le \Delta T_F$. The solution adopted was to utilize a variance-weighted mean wavelength over the bands of interest (wavelength is a time in this context):

$$\tau_{v,\ell} = \frac{\int \frac{1}{\omega} \hat{f}(\omega) d\omega}{\int \hat{f}(\omega) d\omega} \equiv \frac{\int \lambda \hat{f}(\lambda) d\lambda}{\int \hat{f}(\lambda) d\lambda}.$$

The results are also listed in Tables 2 and 3. Herein lies the difference between winter and summer cases: statistically a highly significant difference in the means for all the bands measured, although the separation was not considered such as to justify separate seasonal parametrization. The timescales look eminently suitable in terms of size for the mesoscale, regional and global versions of NAME.

The R91/ADMS formula for low frequency fluctuations, derived from Moore, is

$$\sigma_\theta = 0.065 \left(\frac{7}{u_{10}} T_A \right)^{1/2},$$

where T_A is an averaging time, which rearranges to $\sigma_v^2 = 0.03 u_{10} T_A$. It was decided to seek a parametrization of the form

$$\sigma_{v,\ell}^2 = 2 c_\ell u_{10} \Delta T_F$$

where c_ℓ is a coefficient refined from 0.03 using the computed global, regional and mesoscale variances and the monthly mean wind strengths. The use of a non-constant variance in a random walk technique can in theory lead to particle-

collection problems, but it is expected the impact would be negligible in the NAME model due to the small size of the horizontal gradients in the 10m wind, and the constant changes in time and space. The overall mean wind was 4.8 ms^{-1}, for which $c_\ell = 0.03$ would yield global, regional and mesoscale variances of 1.73, 0.86 and 0.29 m^2s^{-2} respectively.

The c_ℓ are listed in Tables 2 and 3. The most notable results are that the c_ℓ coefficient (for the ensemble) closely approximates the ADMS value of 0.03 at mesoscale, and that it varies with the time resolution. Thus it is reduced for the regional and moreso for the global grid, for which $c_\ell \approx 0.02$. This is a welcome finding, as the global diffusion with meander seemed excessive compared with the other resolutions. The reduction is not great, however, as the spread will be proportional only to the square root of c_ℓ.

It has been suggested (Prof. J.C.R.Hunt, private communication), and seems plausible on dimensional grounds, that for the -5/3 spectral range the velocity variance may be proportional to $T^{2/3}$, implying a constant c_ℓ. Although the average value of c_ℓ computed in this way is roughly equal for the 12 and 6 hr timescales (for summer, winter and the April/September cases---see Table 4) the 2 hr scale shows a fall-off in magnitude which is particularly large for the winter months. The reason for this is not clear, although the seasonal difference may be related to more prevalent unstable conditions in summer and stable conditions in winter. The coefficient c_ℓ is derived from the measured $\sigma^2_{v,\ell} / u$; energy gain or loss due to interaction with buoyancy certainly influences vertical spectra, and where the eddies have a vertical component---i.e. at the high frequency end of the range of interest here---the horizontal (and hence $\sigma^2_{v,\ell}$) will also be affected (see Vinnichenko et al 1980 for some discussion). Compared with summer, winter combines reduced variance below 2 hr with stronger winds in these statistics.

Table 3 summarises the results which form the basis of the NAME parametrization---it is not considered that a breakdown of the parametrization by season is justifiable computationally, in view of the similarities of the mean statistics. The changes in velocity variance and timescale when analysed over the various wavebands for individual months, and the intercomparison of months dominated by particular synoptic types, are of considerable interest, and it was thought worthwhile to make a permanent record of the results for all 27 months for future reference. Tables 5, 6, 7 and 8 contain the statistics for the summer, September, winter and April cases respectively.

Method of Parametrization. The formulation for cross-wind turbulent diffusion is

$$v'_t = v'_{t-1}\left(1 - \frac{\Delta t}{\tau}\right) + \left(\frac{2\sigma_v^2 \Delta t}{\tau}\right)^{1/2} r_t \qquad (1)$$

which reflects only the small scales. Including the component for low frequency wind fluctuations should, perhaps, ideally lead to a higher order stochastic process, autoregressive or integrated, but a simpler solution is to treat the two components as additive (they are statistically independent, and it seems reasonable given their spectral separation). Thus we use (1) with the currently prescribed σ_v's and τ's, and compute a parallel time series from

$$v'_{\ell,t} = v'_{\ell,t-1}\left(1-\frac{\Delta t}{\tau_\ell}\right)+\left(\frac{2\sigma^2_{v,\ell}\Delta t}{\tau_\ell}\right)^{1/2} r_{t,\ell} \qquad (2)$$

where $\sigma_{v,\ell}$ and τ_ℓ are defined as above. Then ultimately the advection velocity, V, is from

$$V_{total} = (V_t + v'_t + v'_{\ell,t}).$$

The problem of applying this parametrization in a model resolved in u and v directions remains. Options are to compute the direction of the wind vector in order to apply $\sigma_{v,\ell}$, to assume $\sigma_{u,\ell}$ is identical to $\sigma_{v,\ell}$ and apply the random walk to both components, or to make a further analysis to investigate the magnitudes of $\sigma_{u,\ell}$. For the present the second of the options is being used in view of the computational expense of the first, and the time and effort required for the third.

Further questions arise: need a far-field form of the meandering be prescribed, at what stage can it be applied, and what are suitable timesteps? For turbulent diffusion we have the far field expression

$$v'_t = \left(\frac{2\sigma_v^2\tau}{\Delta t}\right)^{1/2} r_t, \qquad (3)$$

where Δt is a fixed timestep of 10 or 15 minutes. Likewise we may write

$$v'_{t,\ell} = \left(\frac{2\sigma^2_{v,\ell}\tau_\ell}{\Delta t}\right)^{1/2} r_{t,\ell} \qquad (4)$$

for the far field meandering. This parabolic K-type diffusion should not be applied too close to the source, however, where the spread is linear in time. For the meandering it is safest to wait until $t \approx 4\tau_\ell$ before switching to the far field diffusion. A suggested procedure is---

1. Near-source: Δt_1 calculated to suit turbulent diffusion formulation, as at present. Use equations (1) and (2).

Figure Captions.

Figure 1: Error (diagrammatic) in the 'local mean' wind obtained by applying a moving average to a sudden change in otherwise steady winds.

Figure 2: As Figure 1, but for a steady wind change taking place over a period identical to the length of a moving average.

Figure 3: As Figure 1, for a moving average applied to wind oscillations following a sine wave.

Figure 4: Sample spectra plotted on log-log axes---November 1988 following processing using (a) 12 hr, (b) 6 hr and (c) 2 hr running means. Note the different scale for (a). The vertical axis is spectral density $\hat{f}$, the horizontal i, where $\omega_i = 2\pi i / L$.

Figure 5: Plan view of instantaneous plume at 12, 24, 36 and 48 hr after the commencement of a continuous hypothetical boundary layer release from a point near Aberdeen, as simulated by the NAME dispersion model. Figures 5a, b and c illustrate the effect of including meandering for the global, regional and mesoscale versions respectively. The release commenced 00UTC 30th December 1996. Note that the mesoscale plume is terminated at the boundary of the mesoscale domain.

Figure 6a,b,c: as Figure 4 for a release in the NW of England commencing 00UTC 1st January 1997. Figure 6d is the same run with all meandering removed, for comparison.

Figure7: As Figure 4 for a release at Ascot, commencing 12UTC 30th December 1996.

time resolution of the global, regional and mesoscale versions of the model. The results of applying the scheme have been illustrated and discussed.

The parametrization adopted was to assume $\sigma_{v,\ell}^2 = 2c_\ell u_{10}\Delta T_F$; the coefficient c_ℓ was found to vary with ΔT_F, approximating to the 0.03 of the ADMS scheme only for the mesoscale. Although a number of individual months gave a near-constant c_ℓ on the assumption that the variance is proportional to a two-thirds power of time (as may be justified on dimensional grounds), the ensemble statistics did not sufficiently support the assumption, the mesoscale coefficient for winter cases in particular being much too small.

Acknowledgement: Thanks are due to David Thomson for commenting on the first draft of this paper and to Alison Malcolm for producing Figures 5 to 7.

References:

Davies, B M & Thomson, D J (1995), 'Verification of some turbulence parametrizations', Met O APR Turbulence & Diffusion Note No 223.

Maryon, R H, Saltbones, J, Ryall, D B, Bartnicki, J, Jakobsen, H A & Berge, E (1996), 'An intercomparison of three long range dispersion models developed for the UK Meteorological Office, DNMI and EMEP', Met O APR Turbulence & Diffusion Note No 234.

Moore, D J (1974), 'Observed and calculated magnitudes and distances of maximum ground level concentration of gaseous effluent material downwind of a tall stack', *Adv. Geophys.*, **18B,** 201-221.

Moore, D J (1976), 'Calculation of ground level concentration for different sampling periods and source locations', Atmospheric Pollution, Elsevier.

Physick, W L & Maryon, R H (1995), 'Near-source turbulence parametrization in the NAME model', Met O APR Turbulence & Diffusion Note No 218.

Ryall, D B & Maryon, R H (1996), 'The NAME 2 Dispersion Model: A Scientific Overview', Met O APR Turbulence & Diffusion Note No 217b.

Vinnichenko, N K, Pinus, N Z, Shmeter, S M & Shur, G N (1980), 'Turbulence in the Free Atmosphere', Trans. F L Sinclair, Consultants Bureau, New York.

2. Switch to the turbulent far field in usual way after (it is suggested) 1hr in convective conditions, half an hour for stable, ensuring that $\Delta t_2 << \tau_\ell$, say $\tau_\ell / 10$, i.e. about 6 to 10 minutes for mesoscale. Use equations (3) and (2).

3. Switch to meandering far field after $4\tau_\ell$ with $\Delta t_3 = 10 - 15\text{min}$. Use equations (3) and (4).

It remains to be seen to what extent step 3 is necessary for computational economy.

Application. Figures 5a-5c, 6a-6c and 7a-7c illustrate the application of the parametrization in parallel global, regional and mesoscale runs of the NAME 2.3 model (Figure 6d is a regional run with meander removed completely, for comparison). Each figure shows a plan view of the plume at 12, 24, 36 and 48 hr from the start of a continuous boundary layer release. The far-field homogeneous turbulent diffusion was used, with the meander scheme (equation 2)---it was not necessary to apply the near-source homogeneous and inhomogeneous diffusion schemes for a simple comparison of the meandering at different resolutions. In general, the global results exhibit slightly more diffusive spread than the regional, and both considerably more spread than the mesoscale.

This highlights the difference between resolved and parametrized motions: compare, for example, the situation at 48 hr in Figures 5a, b and c. Where the global and regional parametrizations have simply broadened the plume, the mesoscale has retained a thinner plume but resolved some broader structures absent from the coarse resolutions. To a lesser extent, similar considerations apply in comparisons of the global and regional spreads--- see Figures 6a, 6b at 36 hr, for example. Mostly, however, the mesoscale plume has remained thin compared with the others, and although the mesoscale grid can demonstrably resolve structures of the relevant scales, it may be that in many cases they are not generated in the course of the numerical weather prediction model integrations. On the other hand, the coarser resolutions, by applying a straight diffusion based upon long-term averages, will also be subject to error in a given realization. The optimal strategy to adopt remains to be determined, although it has been observed that NAME requires more rather than less diffusion in long range integrations to obtain the best comparisons with measurements. The conventional statistical comparisons may, however, simply reflect the poor results which can be obtained when a well structured plume simulation is slightly out of phase with the real one. Extra diffusion might be statistically beneficial at the expense of blurring plume structure.

Summary. Twenty-seven months of 10-minute mean surface winds measured at MRU Cardington have been processed with a view to improving the parametrization of meander in the NAME dispersion model. The inherent difficulties have been discussed, and the solution adopted of defining a varying mean wind by means of a moving average. The cross-wind component was computed with reference to the mean wind so defined, and a spectral analysis carried out to determine the cross-wind variance and corresponding timescales for application to the 'spectral gap' between the turbulence parametrization and the

	12 hr		6 hr		2 hr	
	Mean	S.D.	Mean	S.D.	Mean	S.D.
$\sigma^2_{v,\ell}$	1.060	0.196	.6887	0.109	.3107	0.049
$\tau_{v,\ell}$	252.6	11.42	161.8	4.30	63.0	1.40
c_ℓ	.0221	.0040	.0289	.0055	.0387	.0066

Table 2.1 Mean and S.D. of variance, timescale and c_ℓ coefficient for 8 summer cases (May-Aug).

	12 hr		6 hr		2 hr	
	Mean	S.D.	Mean	S.D.	Mean	S.D.
$\sigma^2_{v,\ell}$	1.338	0.497	.7873	0.288	.2837	0.085
$\tau_{v,\ell}$	280.6	13.57	180.6	7.57	71.4	2.37
c_ℓ	.0196	.0037	.0231	.0037	.0251	.0036

Table 2.2 Mean and S.D. of variance, timescale and c_ℓ coefficient for 13 winter cases (Oct-Mar).

	12 hr		6 hr		2 hr	
	Mean	S.D.	Mean	S.D.	Mean	S.D.
$\sigma^2_{v,\ell}$	1.019	0.406	.6766	0.278	.2919	0.104
$\tau_{v,\ell}$	251.5	18.90	164.6	10.58	65.7	1.96
c_ℓ	.0196	.0056	.0260	.0077	.0332	.0078

Table 2.3 Mean and S.D. of variance, timescale and c_ℓ coefficient for 6 Apr and Sep cases.

	12 hr	6 hr	2 hr
$\sigma^2_{v,\ell}$	1.199	.7380	.2972
$\tau_{v,\ell}$ **	266.6	171.2	67.2
c_ℓ	.0209	.0260	.0319

*Table 3. Overall means of variance, timescale and c_ℓ coefficient giving equal weight to winter & summer cases (Apr and Sep results omitted, but are not inconsistent). **N.B. Values of 260, 170 and 60min used in the NAME parametrization for the three resolutions: see page 5.*

	12 hr		6 hr		2 hr	
	Mean	SD	Mean	SD	Mean	SD
Summer	.0506	.0091	.0525	.0099	.0488	.0083
Winter	.0449	.0084	.0420	.0068	.0316	.0045
Apr/Sep	.0448	.0129	.0472	.0139	.0418	.0098

Table 4. Mean and S.D. of c_ℓ coefficient calculated on the assumption that $\sigma^2_{v,\ell} \propto T_F^{2/3}$.

The units for Tables 2 to 4 are--- $\sigma^2_{v,\ell}$: $m^2 s^{-2}$, $\tau_{v,\ell}$: min. and c_ℓ: $ms^{-1} hr^{-1}$.

Period 20min to:	$\sigma^2_{v,\ell}$ (m^2s^{-2}) 12hr	6hr	2hr	$\tau_{v,\ell}$ (min) 12hr	6hr	2hr	c_ℓ $(ms^{-1}\,hr^{-1})$ 12hr	6hr	2hr
11.1hr	1.079			263.1			.0167		
6.67hr	.6986	.6942		159.7	165.9			.0214	
3.33hr	.3885	.3941		89.8	89.6				
2.08hr	.2609	.2651	.2913	60.7	61.1	63.9			.0267
1.01hr	.1316	.1332	.1306	37.2	37.2	36.5			

Table 5.1 Variance, timescale and c_ℓ coefficient for Jul 1988 (4000 10-minute means, $u_{10}=5.40ms^{-1}$).

Period 20min to:	$\sigma^2_{v,\ell}$ (m^2s^{-2}) 12hr	6hr	2hr	$\tau_{v,\ell}$ (min) 12hr	6hr	2hr	c_ℓ $(ms^{-1}hr^{-1})$ 12hr	6hr	2hr
11.1hr	.9244			258.9			.0169		
6.67hr	.6040	.5781		150.9	156.5			.0211	
3.33hr	.3479	.3407		87.0	84.2				
2.08hr	.2460	.2514	.2787	60.9	61.5	65.0			.0303
1.01hr	.1273	.1293	.1242	37.0	36.9	36.4			

Table 5.2 Variance, timescale and c_ℓ coefficient for Aug 1988 (4059 10-minute means, $u_{10}=4.56ms^{-1}$).

Period 20min to:	$\sigma^2_{v,\ell}$ (m^2s^{-2}) 12hr	6hr	2hr	$\tau_{v,\ell}$ (min) 12hr	6hr	2hr	c_ℓ $(ms^{-1}hr^{-1})$ 12hr	6hr	2hr
11.1hr	.9818			254.6			.0223		
6.67hr	.6577	.5841		160.8	159.8			.0266	
3.33hr	.3643	.3371		88.4	83.2				
2.08hr	.2472	.2470	.2758	59.9	60.2	63.0			.0372
1.01hr	.1356	.1363	.1376	37.3	37.3	36.8			

Table 5.3 Variance, timescale and c_ℓ coefficient for May 1989 (4400 10-minute means, $u_{10}=3.67ms^{-1}$).

Period	$\sigma^2_{v,\ell}$ (m^2s^{-2}) 12hr	6hr	2hr	$\tau_{v,\ell}$ (min) 12hr	6hr	2hr	c_ℓ $(ms^{-1}\,hr^{-1})$ 12hr	6hr	2hr
11.1hr	1.049			238.4			.0258		
6.67hr	.7256	.7394		154.8	165.1			.0364	
3.33hr	.4257	.4111		84.6	82.2				
2.08hr	.2962	.2958	.3132	57.7	57.9	60.5			.0459
1.01hr	.1690	.1693	.1635	37.2	37.2	36.4			

Table 5.4 Variance, timescale and c_ℓ coefficient for Jun 1989 (3756 10-minute means, $u_{10}=3.38ms^{-1}$).

Period 20min to:	$\sigma^2_{v,\ell}$ (m^2s^{-2}) 12hr	6hr	2hr	$\tau_{v,\ell}$ (min) 12hr	6hr	2hr	c_ℓ $(ms^{-1}hr^{-1})$ 12hr	6hr	2hr
11.1hr	.7115			238.0			.0227		
6.67hr	.4811	.5265		149.9	166.6			.0334	
3.33hr	.2871	.2829		84.0	83.2				
2.08hr	.2070	.2080	.2321	59.6	60.5	63.9			.0439
1.01hr	.1160	.1147	.1123	37.3	37.2	36.3			

Table 5.5 Variance, timescale and c_ℓ coefficient for Jul 1989 (4430 10-minute means, $u_{10}=2.62ms^{-1}$).

Period 20min to:	$\sigma^2_{v,\ell}$ (m^2s^{-2}) 12hr	6hr	2hr	$\tau_{v,\ell}$ (min) 12hr	6hr	2hr	c_ℓ $(ms^{-1}\ hr^{-1})$ 12hr	6hr	2hr
11.1hr	1.402			273.1			.0289		
6.67hr	.8483	.8377		159.9	166.0			.0344	
3.33hr	.4549	.4590		86.0	84.9				
2.08hr	.3248	.3329	.3519	60.7	61.2	64.0			.0431
1.01hr	.1731	.1755	.1673	37.6	37.5	37.0			

Table 5.6 Variance, timescale and c_ℓ coefficient for Jun 1990 (3310 10-minute means, $u_{10}=4.05ms^{-1}$).

Period 20min to:	$\sigma^2_{v,\ell}$ (m^2s^{-2}) 12hr	6hr	2hr	$\tau_{v,\ell}$ (min) 12hr	6hr	2hr	c_ℓ $(ms^{-1}\ hr^{-1})$ 12hr	6hr	2hr
11.1hr	1.272			247.9			.0240		
6.67hr	.8575	.8292		152.1	155.7			.0312	
3.33hr	.4959	.4943		84.2	82.8				
2.08hr	.3531	.3611	.3940	58.4	59.4	61.4			.0442
1.01hr	.1992	.1992	.2003	37.5	37.4	36.6			

Table 5.7 Variance, timescale and c_ℓ coefficient for Jul 1990 (3557 10-minute means, $u_{10}=4.42ms^{-1}$).

Period	$\sigma^2_{v,\ell}$ (m^2s^{-2}) 12hr	6hr	2hr	$\tau_{v,\ell}$ (min) 12hr	6hr	2hr	c_ℓ $(ms^{-1}\ hr^{-1})$ 12hr	6hr	2hr
11.1hr	1.062			247.0			.0196		
6.67hr	.7176	.7206		151.8	158.6			.0267	
3.33hr	.4086	.4150		79.9	80.5				
2.08hr	.3097	.3116	.3484	58.8	59.7	62.6			.0383
1.01hr	.1727	.1704	.1701	37.1	37.0	36.6			

Table 5.8 Variance, timescale and c_ℓ coefficient for Aug 1990 (4460 10-minute means, $u_{10}=4.51ms^{-1}$).

Period 20min to:	$\sigma^2_{v,\ell}$ (m^2s^{-2}) 12hr	6hr	2hr	$\tau_{v,\ell}$ (min) 12hr	6hr	2hr	c_ℓ $(ms^{-1}\,hr^{-1})$ 12hr	6hr	2hr
11.1hr	1.062			246.2			.0193		
6.67hr	.6384	.6280		143.2	146.2			.0229	
3.33hr	.4111	.4198		88.7	87.6				
2.08hr	.2909	.3057	.3386	64.1	65.4	68.1			.0367
1.01hr	.1395	.1424	.1389	38.2	38.0	37.1			

Table 6.1 Variance, timescale and c_ℓ coefficient for Sep 1988 (4072 10-minute means, $u_{10}=4.57ms^{-1}$).

Period 20min to:	$\sigma^2_{v,\ell}$ (m^2s^{-2}) 12hr	6hr	2hr	$\tau_{v,\ell}$ (min) 12hr	6hr	2hr	c_ℓ $(ms^{-1}hr^{-1})$ 12hr	6hr	2hr
11.1hr	.5204			259.4			.0183		
6.67hr	.3618	.3457		160.5	163.4			.0243	
3.33hr	.2052	.2020		96.6	95.7				
2.08hr	.1314	.1312	.1416	64.8	65.8	66.5			.0296
1.01hr	.0619	.0606	.0606	37.6	37.5	37.2			

Table 6.2 Variance, timescale and c_ℓ coefficient for Sep 1989 (4240 10-minute means, $u_{10}=2.36ms^{-1}$).

Period 20min to:	$\sigma^2_{v,\ell}$ (m^2s^{-2}) 12hr	6hr	2hr	$\tau_{v,\ell}$ (min) 12hr	6hr	2hr	c_ℓ $(ms^{-1}\,hr^{-1})$ 12hr	6hr	2hr
11.1hr	1.300			272.1			.0232		
6.67hr	.8197	.8053		166.0	170.5			.0288	
3.33hr	.4227	.4288		88.9	86.6				
2.08hr	.2938	.3078	.3357	62.3	63.1	65.8			.0357
1.01hr	.1466	.1506	.1454	38.0	38.1	37.2			

Table 6.3 Variance, timescale and c_ℓ coefficient for Sep 1990 (4320 10-minute means, $u_{10}=4.66ms^{-1}$).

Period 20min to:	$\sigma^2_{v,\ell}$ (m^2s^{-2}) 12hr	6hr	2hr	$\tau_{v,\ell}$ (min) 12hr	6hr	2hr	c_ℓ $(ms^{-1}\,hr^{-1})$ 12hr	6hr	2hr
11.1hr	1.755			285.8			.0242 .		
6.67hr	.9363	1.026		164.0	179.5			.0283	
3.33hr	.5001	.5123		93.7	92.8				
2.08hr	.3336	.3467	.3914	66.7	66.9	71.6			.0321
1.01hr	.1441	.1461	.1420	38.6	38.2	37.8			

Table 7.1 Variance, timescale and c_ℓ coefficient for Feb 1988 (3545 10-minute means, $u_{10}=6.03ms^{-1}$).

Period 20min to:	$\sigma^2_{v,\ell}$ (m^2s^{-2}) 12hr	6hr	2hr	$\tau_{v,\ell}$ (min) 12hr	6hr	2hr	c_ℓ $(ms^{-1}\,hr^{-1})$ 12hr	6hr	2hr
11.1hr	1.673			296.5			.0241		
6.67hr	.9207	.9293		177.4	185.7			.0267	
3.33hr	.4415	.4519		96.4	97.1				
2.08hr	.2759	.2809	.3181	65.0	66.4	69.4			.0271
1.01hr	.1298	.1283	.1269	37.8	37.9	37.3			

Table 7.2 Variance, timescale and c_ℓ coefficient for Mar 1988 (4248 10-minute means, $u_{10}=5.80ms^{-1}$).

Period 20min to:	$\sigma^2_{v,\ell}$ (m^2s^{-2}) 12hr	6hr	2hr	$\tau_{v,\ell}$ (min) 12hr	6hr	2hr	c_ℓ $(ms^{-1}\,hr^{-1})$ 12hr	6hr	2hr
11.1hr	1.137			274.0			.0216		
6.67hr	.6814	.7001		168.8	175.3			.0266	
3.33hr	.3608	.3754		95.9	95.5				
2.08hr	.2367	.2476	.2784	67.8	68.6	70.6			.0313
1.01hr	.1019	.1057	.1065	38.2	38.4	37.8			

Table 7.3 Variance, timescale and c_ℓ coefficient for Oct 1988 (4231 10-minute means, $u_{10}=4.40ms^{-1}$).

Period	$\sigma^2_{v,\ell}$ (m^2s^{-2}) 12hr	6hr	2hr	$\tau_{v,\ell}$ (min) 12hr	6hr	2hr	c_ℓ $(ms^{-1}hr^{-1})$ 12hr	6hr	2hr
11.1hr	.6346			253.5			.0161		
6.67hr	.4243	.4175		167.9	179.3			.0212	
3.33hr	.2378	.2220		98.2	98.0				
2.08hr	.1520	.1435	.1723	68.0	69.3	66.1			.0260
1.01hr	.0631	.0581	.0747	38.3	38.8	36.2			

Table 7.4 Variance, timescale and c_ℓ coefficient for Nov 1988 (4180 10-minute means, $u_{10}=3.29ms^{-1}$).

Period	$\sigma^2_{v,\ell}$ (m^2s^{-2})			$\tau_{v,\ell}$ (min)			c_ℓ $(ms^{-1}hr^{-1})$		
20min to:	12hr	6hr	2hr	12hr	6hr	2hr	12hr	6hr	2hr
11.1hr	.8156			272.3			.0125		
6.67hr	.5322	.5208		171.6	178.1			.0159	
3.33hr	.2784	.2740		99.8	98.5				
2.08hr	.1781	.1805	.2105	71.0	72.1	75.0			.0191
1.01hr	.0669	.0662	.0642	39.6	39.6	38.7			

Table 7.5 Variance, timescale and c_ℓ coefficient for Dec 1988 (4400 10-minute means, $u_{10}=5.45ms^{-1}$).

Period	$\sigma^2_{v,\ell}$ (m^2s^{-2})			$\tau_{v,\ell}$ (min)			c_ℓ $(ms^{-1}hr^{-1})$		
20min to:	12hr	6hr	2hr	12hr	6hr	2hr	12hr	6hr	2hr
11.1hr	.8055			264.7			.0145		
6.67hr	.5220	.5158		161.6	169.3			.0187	
3.33hr	.2910	.2882		94.9	95.1				
2.08hr	.1992	.2001	.2154	68.5	70.4	74.1			.0231
1.01hr	.0829	.0787	.0705	38.6	38.7	38.6			

Table 7.6 Variance, timescale and c_ℓ coefficient for Jan 1989 (4190 10-minute means, $u_{10}=4.61ms^{-1}$).

Period	$\sigma^2_{v,\ell}$ (m^2s^{-2})			$\tau_{v,\ell}$ (min)			c_ℓ $(ms^{-1}hr^{-1})$		
20min to:	12hr	6hr	2hr	12hr	6hr	2hr	12hr	6hr	2hr
11.1hr	1.585			277.2			.0202		
6.67hr	.8649	.9051		160.2	171.1			.0230	
3.33hr	.4869	.4978		95.6	95.9				
2.08hr	.3210	.3362	.3659	68.0	70.6	72.9			.0277
1.01hr	.1324	.1260	.1184	39.0	38.7	37.8			

Table 7.7 Variance, timescale and c_ℓ coefficient for Feb 1989 (4010 10-minute means, $u_{10}=6.55ms^{-1}$).

Period	$\sigma^2_{v,\ell}$ (m^2s^{-2})			$\tau_{v,\ell}$ (min)			c_ℓ $(ms^{-1}hr^{-1})$		
	12hr	6hr	2hr	12hr	6hr	2hr	12hr	6hr	2hr
11.1hr	1.266			293.9			.0185		
6.67hr	.6873	.6812		173.7	183.4			.0199	
3.33hr	.3370	.3302		95.2	93.3				
2.08hr	.2187	.2197	.2502	65.6	66.2	69.3			.0217
1.01hr	.1020	.1015	.0993	38.6	38.5	37.8			

Table 7.8 Variance, timescale and c_ℓ coefficient for Oct 1989 (4462 10-minute means, $u_{10}=5.71ms^{-1}$).

Period	$\sigma^2_{v,\ell}$ (m^2s^{-2})			$\tau_{v,\ell}$ (min)			c_ℓ $(ms^{-1}\,hr^{-1})$		
20min to:	12hr	6hr	2hr	12hr	6hr	2hr	12hr	6hr	2hr
11.1hr	1.033			281.7			.0215		
6.67hr	.5951	.6144		181.6	188.8			.0254	
3.33hr	.2899	.2939		100.6	99.3				
2.08hr	.1718	.1771	.1894	67.7	68.1	70.1			.0233
1.01hr	.0733	.0734	.0698	40.2	40.3	39.1			

Table 7.9 Variance, timescale and c_ℓ coefficient for Nov 1989 (4320 10-minute means, $u_{10}=4.02ms^{-1}$).

Period	$\sigma^2_{v,\ell}$ (m^2s^{-2})			$\tau_{v,\ell}$ (min)			c_ℓ $(ms^{-1}hr^{-1})$		
20min to:	12hr	6hr	2hr	12hr	6hr	2hr	12hr	6hr	2hr
11.1hr	.9478			280.1			.0182		
6.67hr	.6146	.5418		175.7	171.9			.0209	
3.33hr	.3051	.3000		98.9	99.2				
2.08hr	.1939	.1918	.2191	69.1	70.1	73.4			.0251
1.01hr	.0778	.0747	.0714	39.2	39.2	38.8			

Table 7.10 Variance, timescale and c_ℓ coefficient for Dec 1989 (3600 10-minute means, $u_{10}=4.33ms^{-1}$).

Period	$\sigma^2_{v,\ell}$ (m^2s^{-2})			$\tau_{v,\ell}$ (min)			c_ℓ $(ms^{-1}\,hr^{-1})$		
20min to:	12hr	6hr	2hr	12hr	6hr	2hr	12hr	6hr	2hr
11.1hr	2.074			307.3			.0252		
6.67hr	1.086	1.154		184.6	196.8			.0280	
3.33hr	.4886	.4973		101.8	100.5				
2.08hr	.2886	.3011	.3350	70.0	69.7	73.8			.0241
1.01hr	.1093	.1136	.1023	40.2	39.8	39.2			

Table 7.11 Variance, timescale and c_ℓ coefficient for Jan 1990 (3578 10-minute means, $u_{10}=6.88ms^{-1}$).

Period	$\sigma^2_{v,\ell}$ (m^2s^{-2})			$\tau_{v,\ell}$ (min)			c_ℓ $(ms^{-1}\,hr^{-1})$		
	12hr	6hr	2hr	12hr	6hr	2hr	12hr	6hr	2hr
11.1hr	2.326			273.2			.0201		
6.67hr	1.456	1.467		179.7	187.7			.0253	
3.33hr	.7212	.6908		100.8	98.3				
2.08hr	.4175	.4234	.4695	65.9	66.7	70.1			.0240
1.01hr	.1778	.1839	.1740	39.4	39.5	38.6			

Table 7.12 Variance, timescale and c_ℓ coefficient for Feb 1990 (4030 10-minute means, $u_{10}=9.67ms^{-1}$).

Period 20min to:	$\sigma^2_{v,\ell}$ (m^2s^{-2}) 12hr	6hr	2hr	$\tau_{v,\ell}$ (min) 12hr	6hr	2hr	c_ℓ $(ms^{-1}\,hr^{-1})$ 12hr	6hr	2hr
11.1hr	1.340			288.1			.0182		
6.67hr	.7512	.7616		171.0	180.3			.0207	
3.33hr	.3756	.3789		94.6	94.5				
2.08hr	.2483	.2533	.2728	66.9	68.5	71.5			.0220
1.01hr	.1089	.1067	.1002	38.5	38.4	37.8			

Table 7.13 Variance, timescale and c_ℓ coefficient for Oct 1990 (4464 10-minute means, $u_{10}=6.14ms^{-1}$).

Period 20min to:	$\sigma^2_{v,\ell}$ (m^2s^{-2}) 12hr	6hr	2hr	$\tau_{v,\ell}$ (min) 12hr	6hr	2hr	c_ℓ $(ms^{-1}hr^{-1})$ 12hr	6hr	2hr
11.1hr	.5736			213.4			.0101		
6.67hr	.3826	.4433		135.6	158.1			.0157	
3.33hr	.2583	.2532		79.4	76.6				
2.08hr	.1955	.1995	.2250	58.7	59.3	62.3			.0236
1.01hr	.1108	.1112	.1101	37.6	37.8	36.6			

Table 8.1 Variance, timescale and c_ℓ coefficient for April 1988 (2073 10-minute means, $u_{10}=4.73ms^{-1}$).

Period 20min to:	$\sigma^2_{v,\ell}$ (m^2s^{-2}) 12hr	6hr	2hr	$\tau_{v,\ell}$ (min) 12hr	6hr	2hr	c_ℓ $(ms^{-1}hr^{-1})$ 12hr	6hr	2hr
11.1hr	.9600			253.2			.0178		
6.67hr	.6508	.6333		163.1	169.4			.0234	
3.33hr	.3635	.3467		93.0	89.6				
2.08hr	.2347	.2390	.2421	61.3	62.4	64.0			.0266
1.01hr	.1195	.1206	.1112	37.2	37.7	36.4			

Table 8.2 Variance, timescale and c_ℓ coefficient for April 1989 (4320 10-minute means, $u_{10}=4.5ms^{-1}$).

Period	$\sigma^2_{v,\ell}$ (m^2s^{-2}) 12hr	6hr	2hr	$\tau_{v,\ell}$ (min) 12hr	6hr	2hr	c_ℓ $(ms^{-1}\,hr^{-1})$ 12hr	6hr	2hr
11.1hr	1.695			264.7			.0287		
6.67hr	1.091	1.204		168.4	179.8			.0408	
3.33hr	.5845	.6227		93.3	93.5				
2.08hr	.3793	.4023	.4685	63.4	64.2	67.2			.0471
1.01hr	.1823	.1901	.1932	38.7	38.6	37.8			

Table 8.3 Variance, timescale and c_ℓ coefficient for April 1990 (3636 10-minute means, $u_{10}=4.93ms^{-1}$).

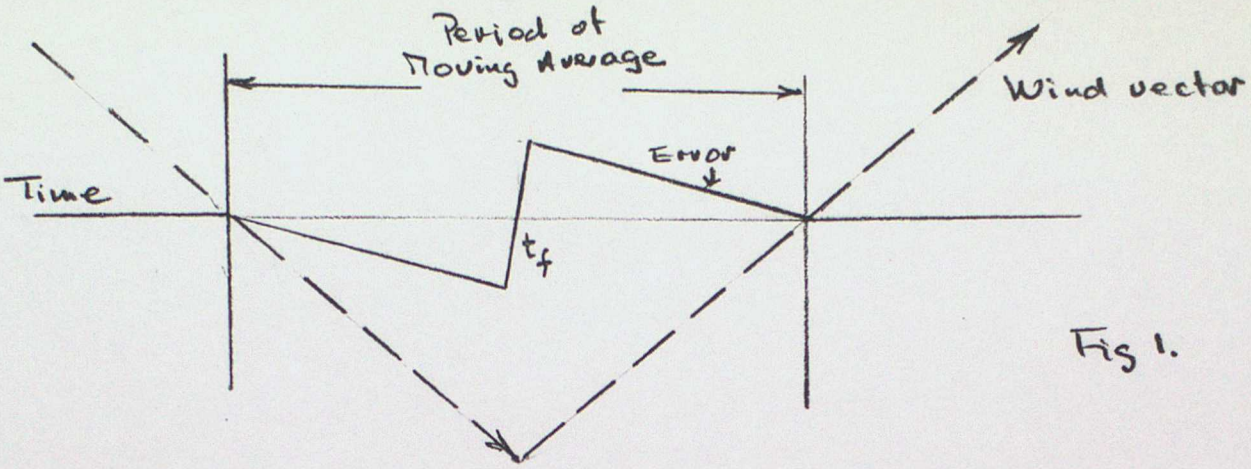

Fig 1.

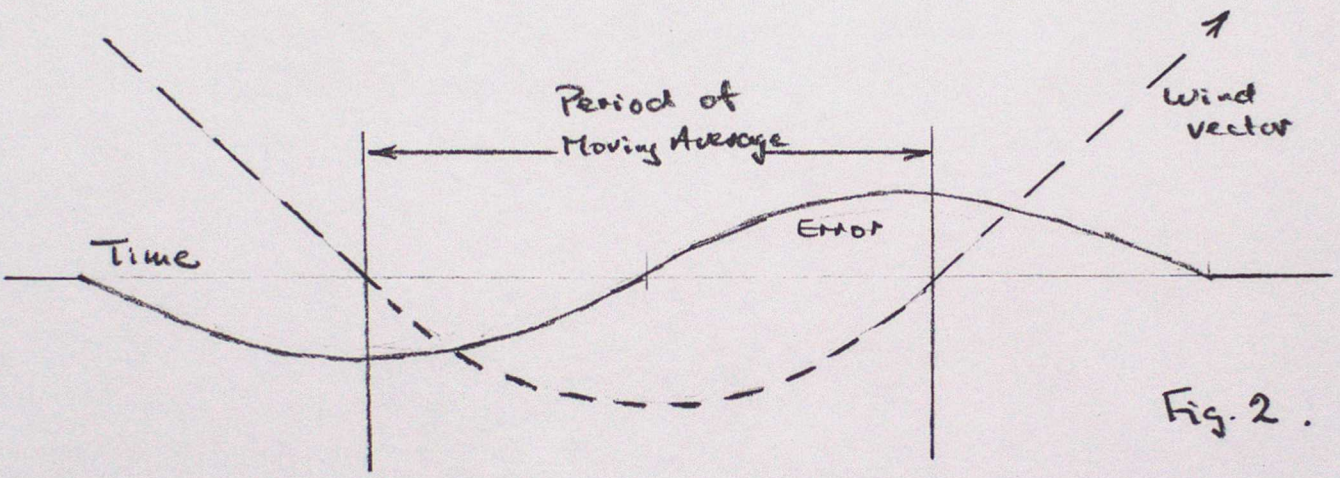

Fig. 2.

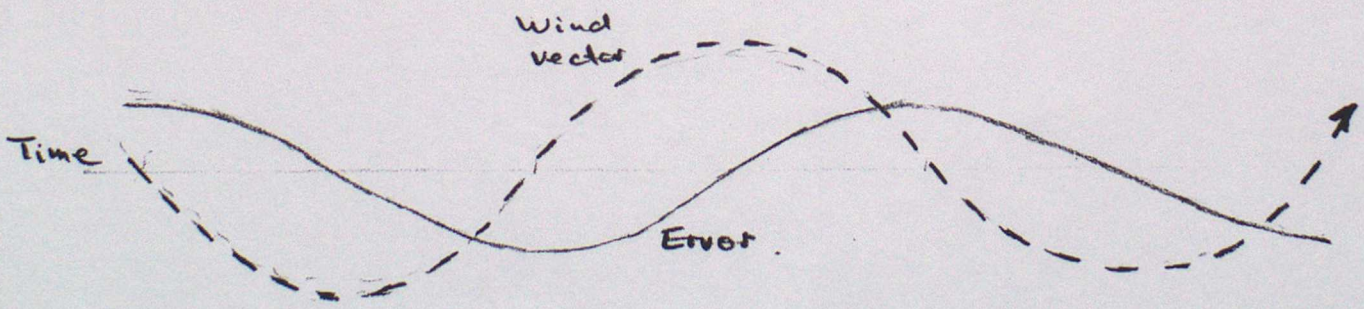

Fig. 3

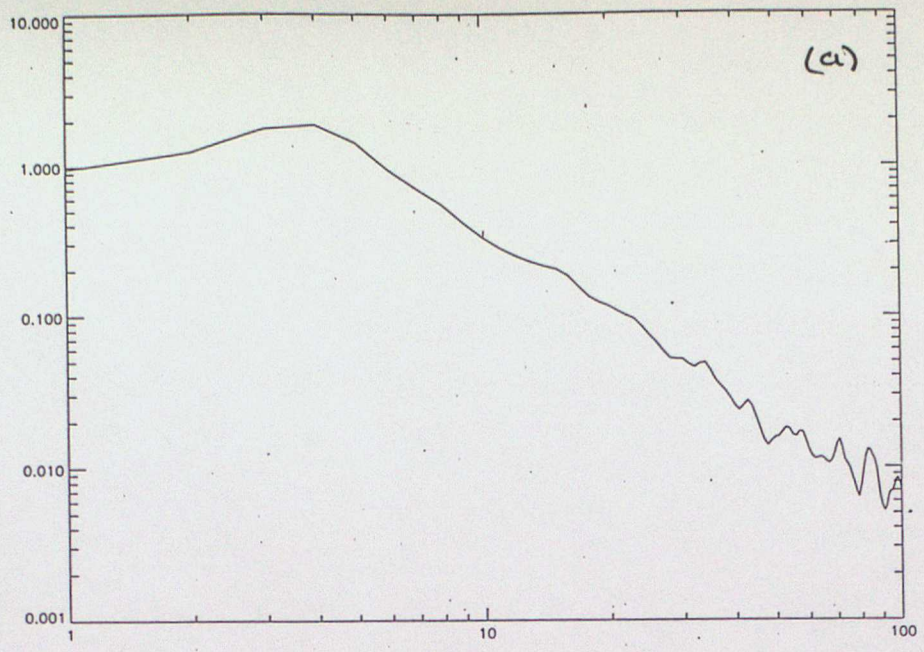
10.000
1.000
0.100
0.010
0.001
1
10
100
(a)

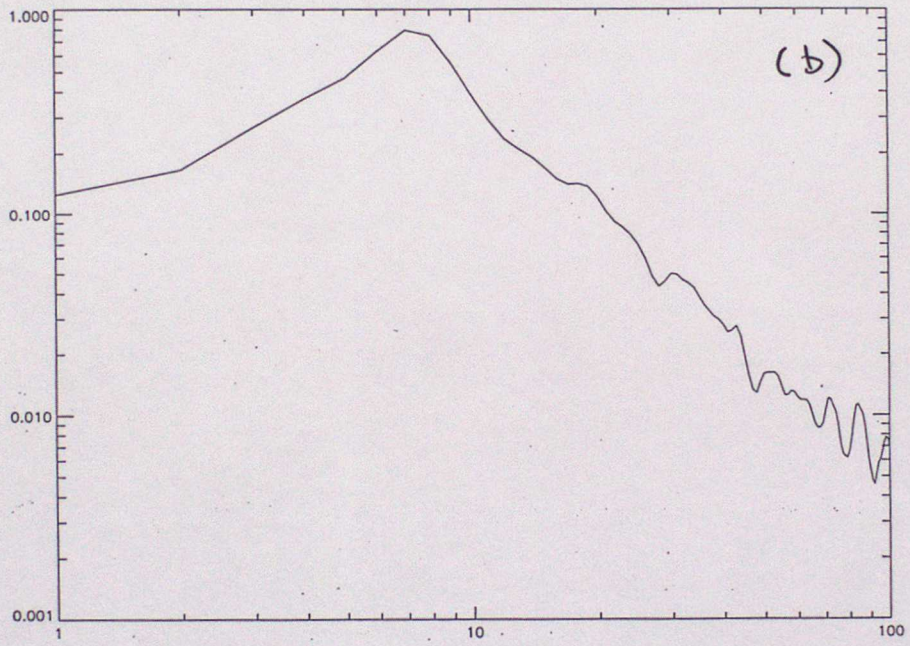
1.000
0.100
0.010
0.001
1
10
100
(b)

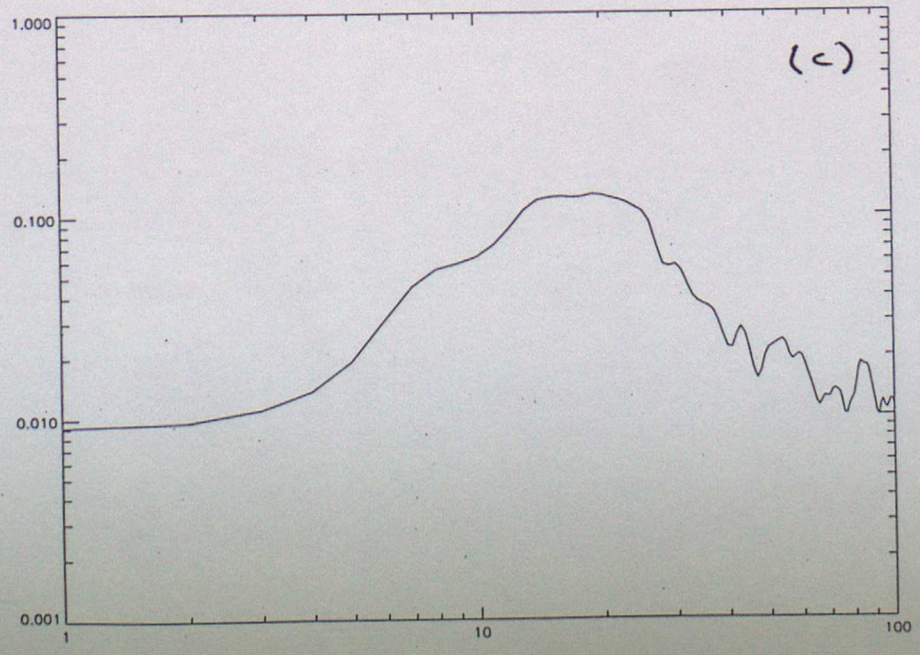
1.000
0.100
0.010
0.001
1
10
100
(c)

Fig 4.

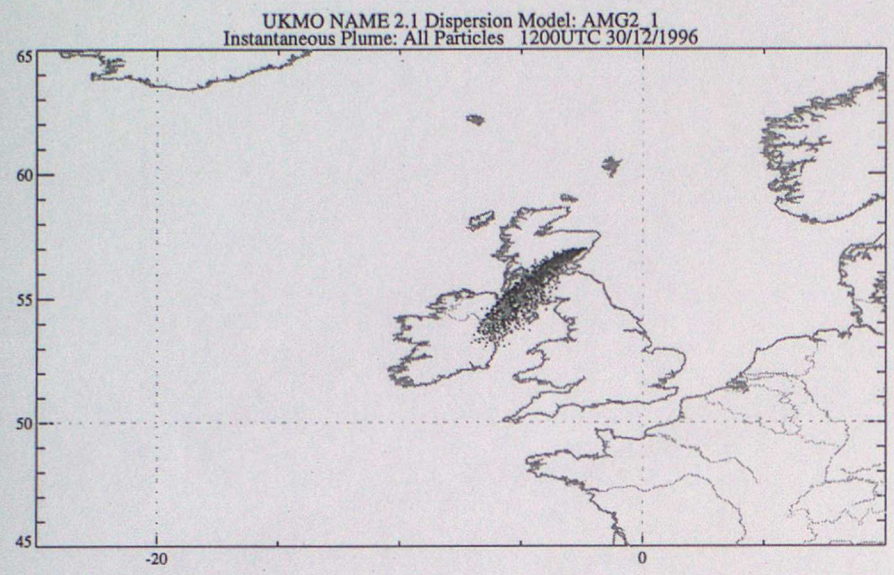

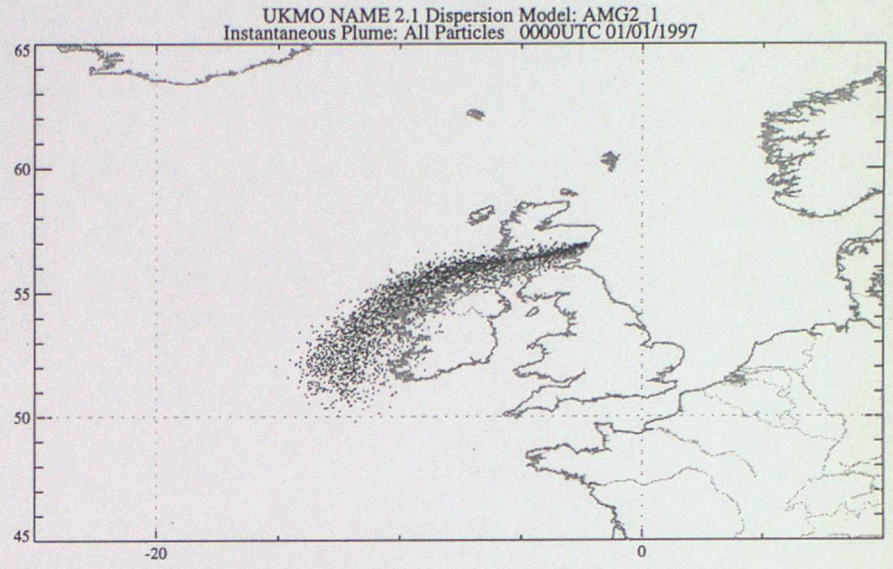

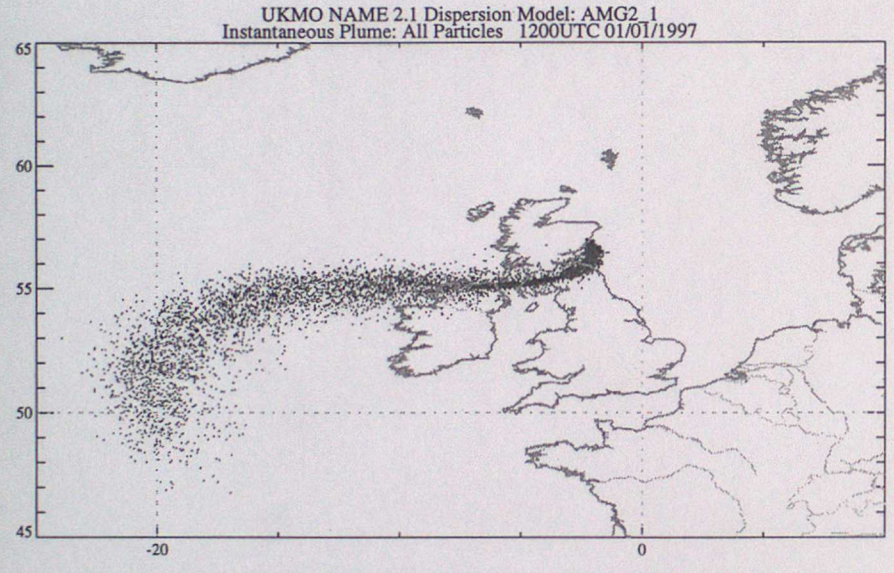

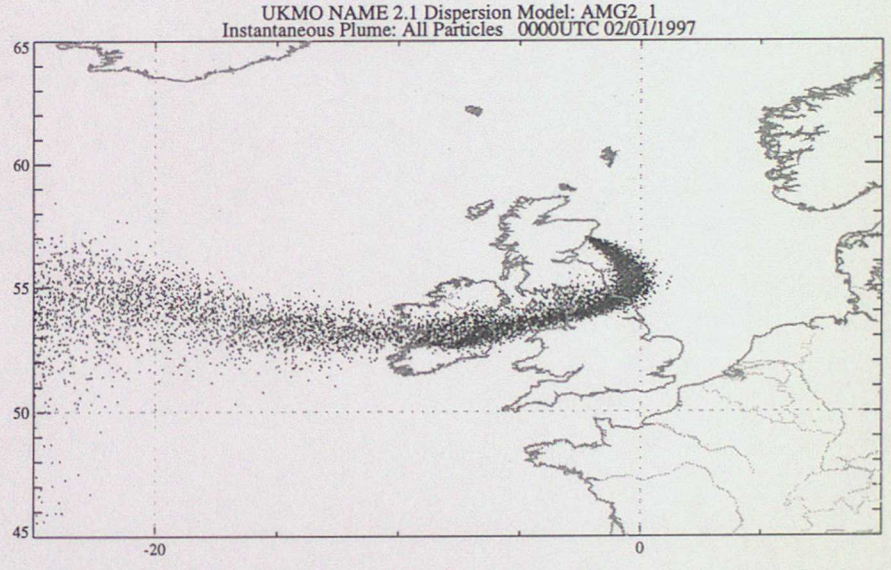

Fig 5a *Global Input*

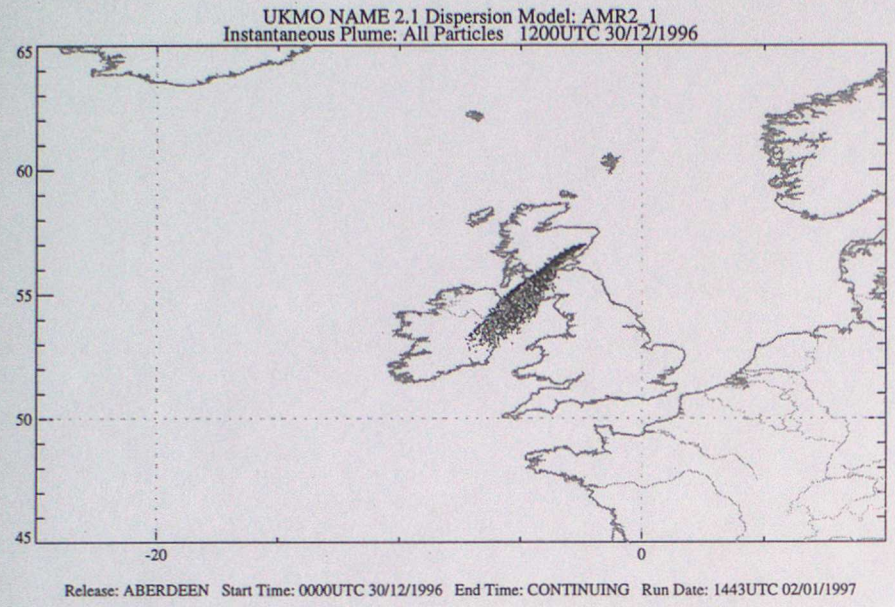

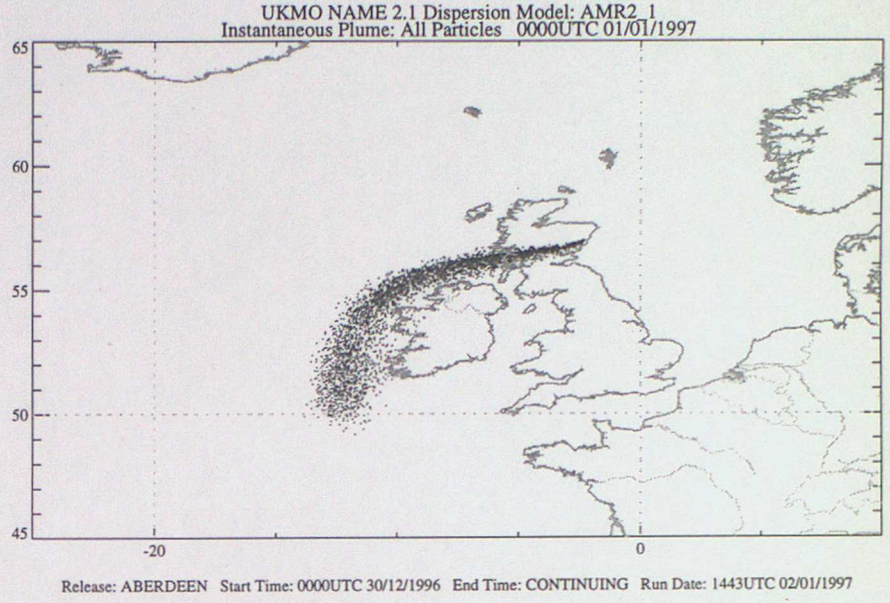

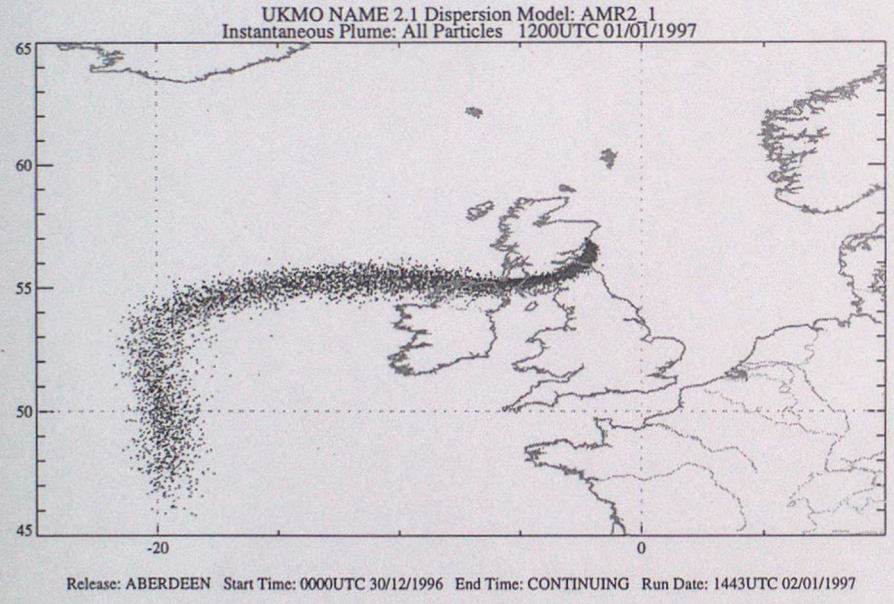

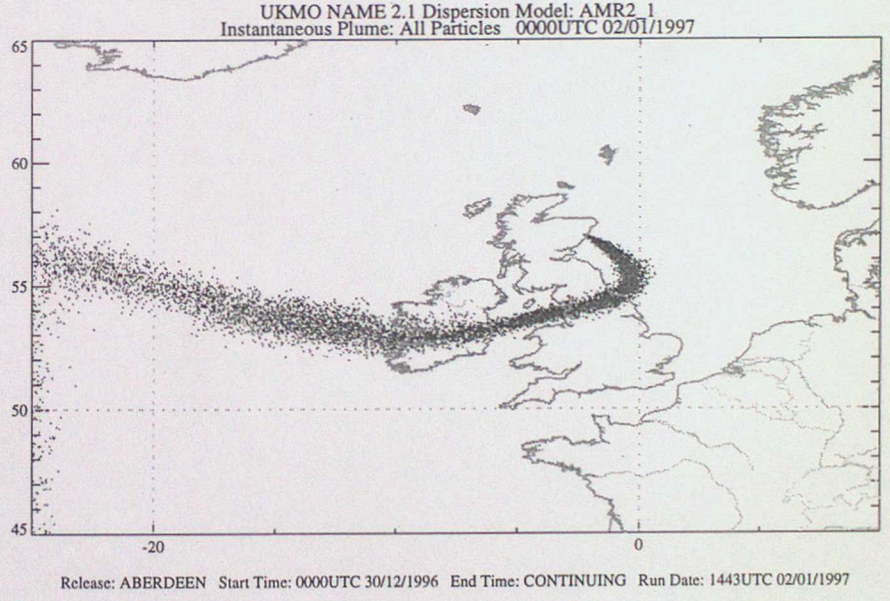

Fig 5b *Regional Input*

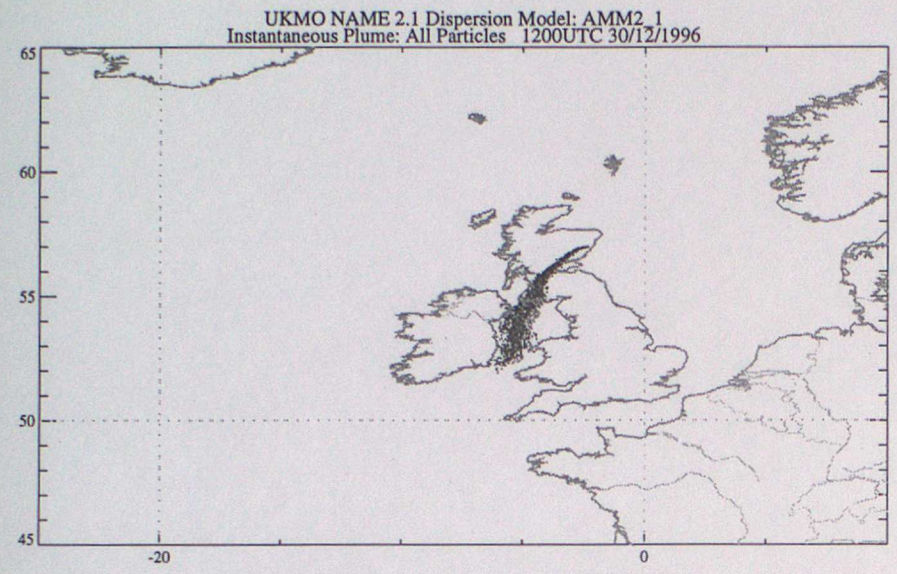

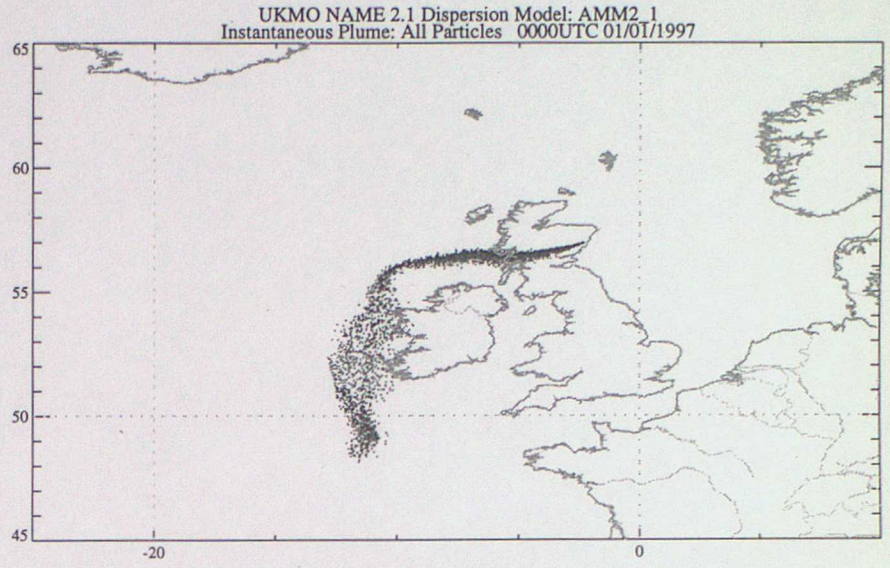

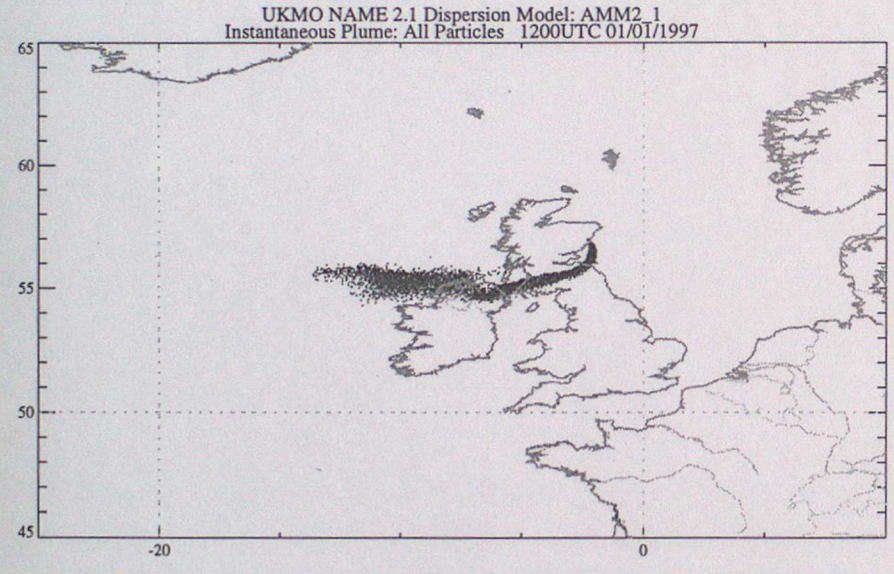

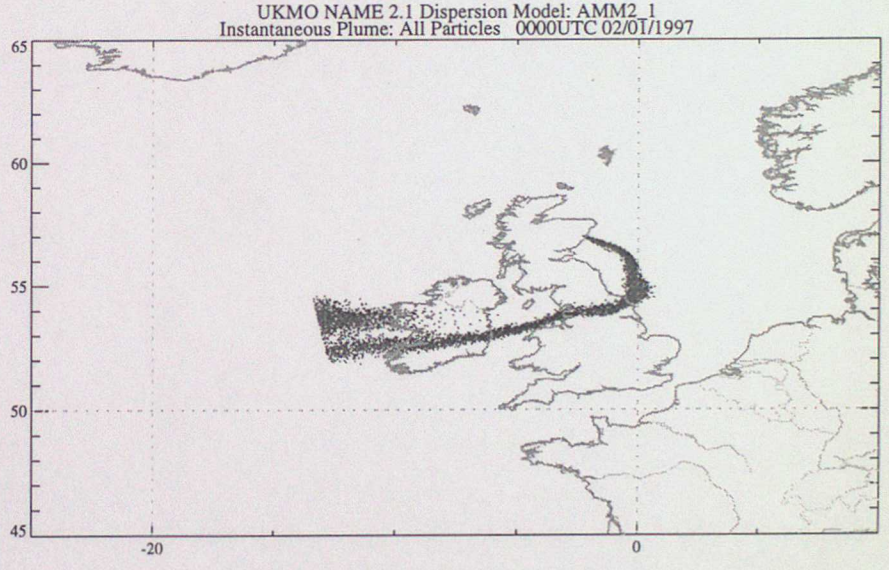

Fig 5c. *Mesoscale Input*

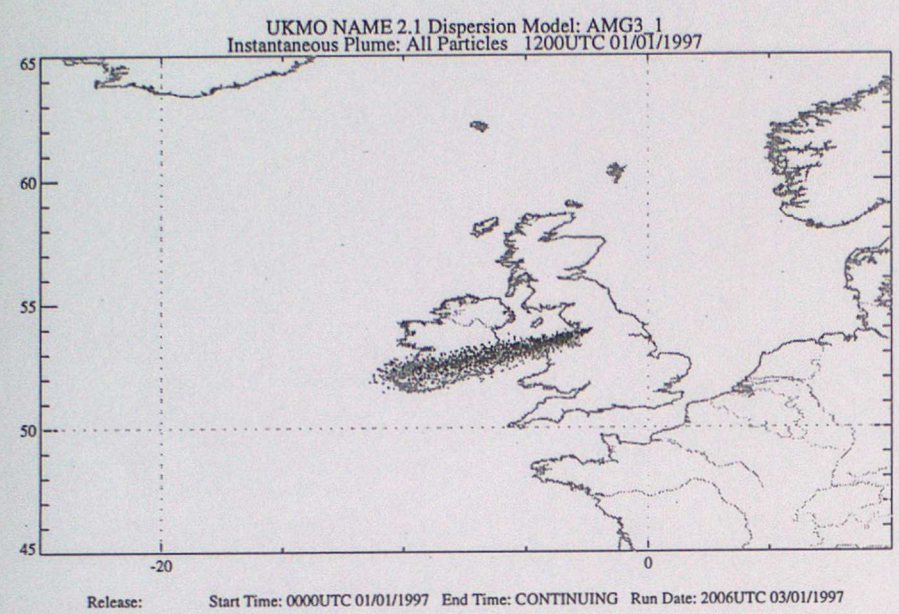

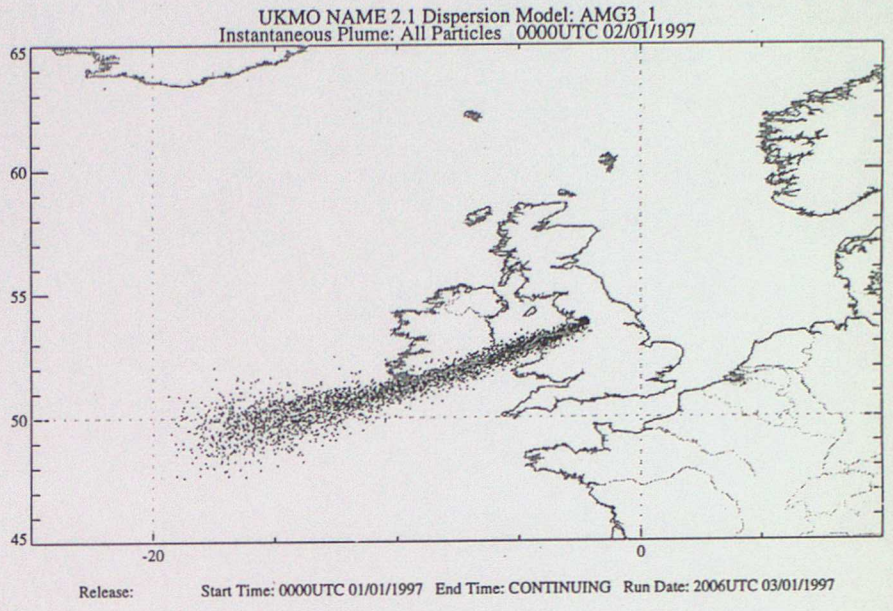

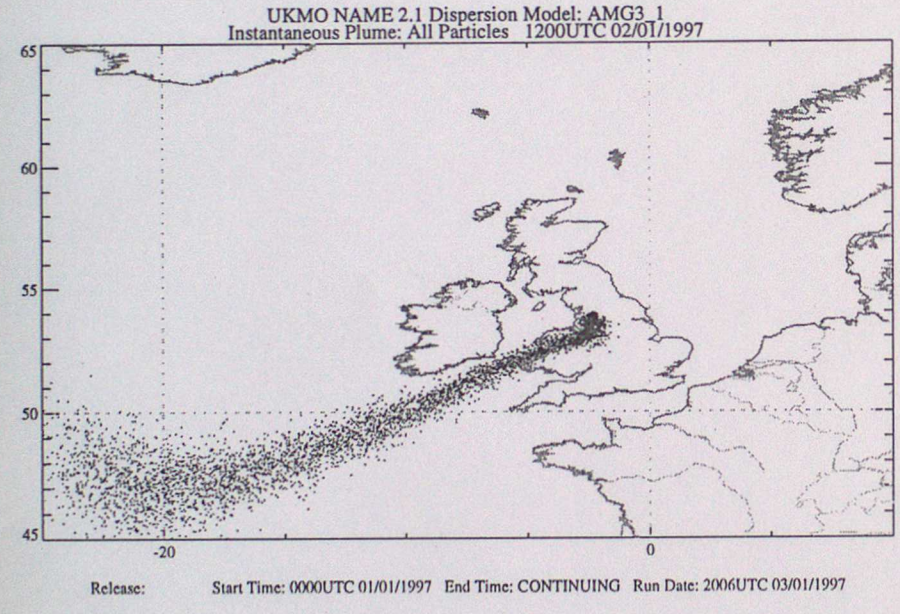

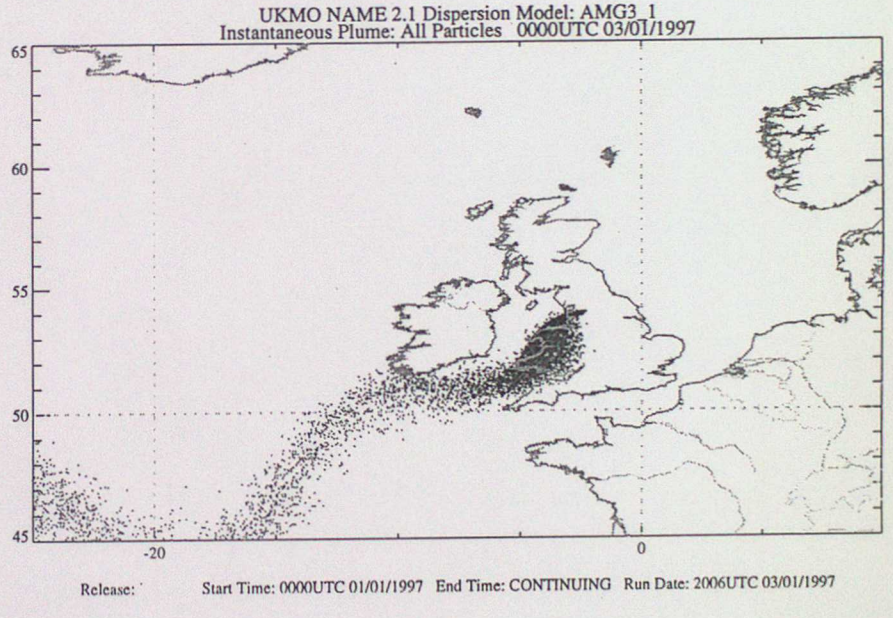

Fig. 6a *Global Input*

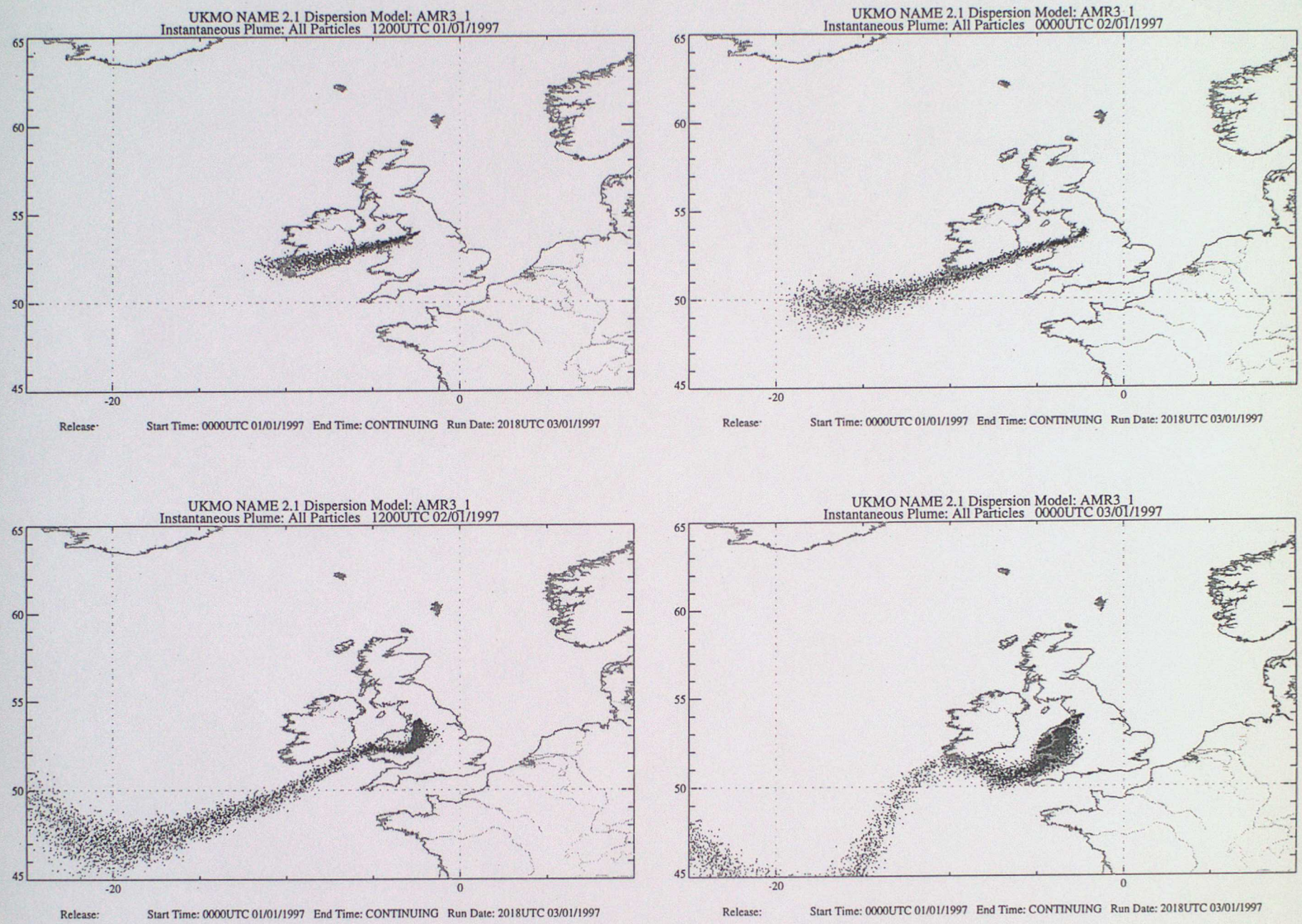

Fig 6b. *Regional Input*

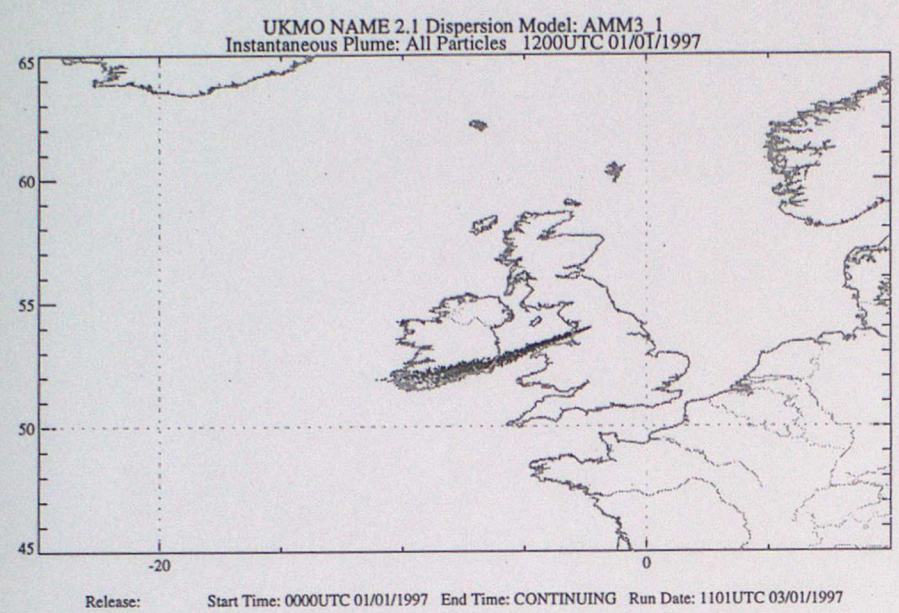

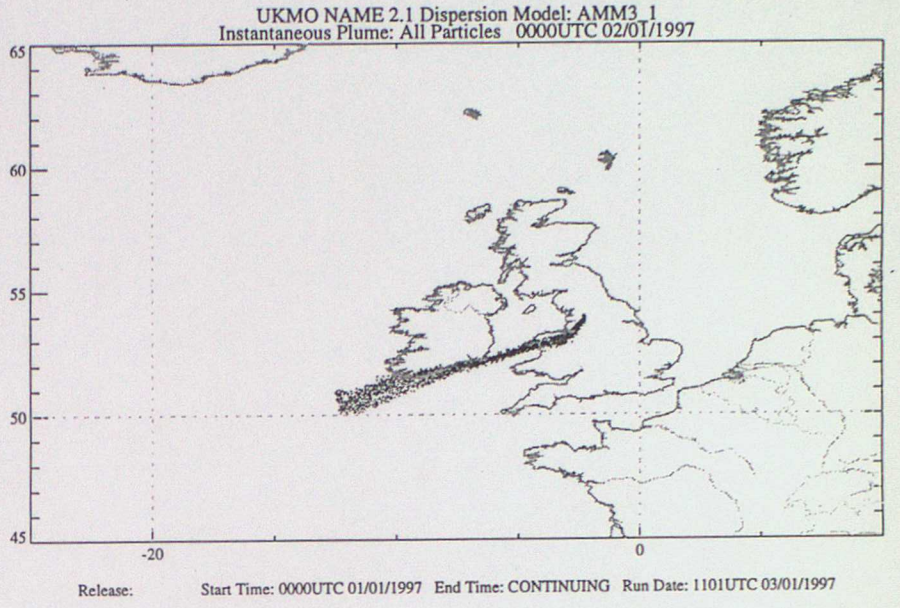

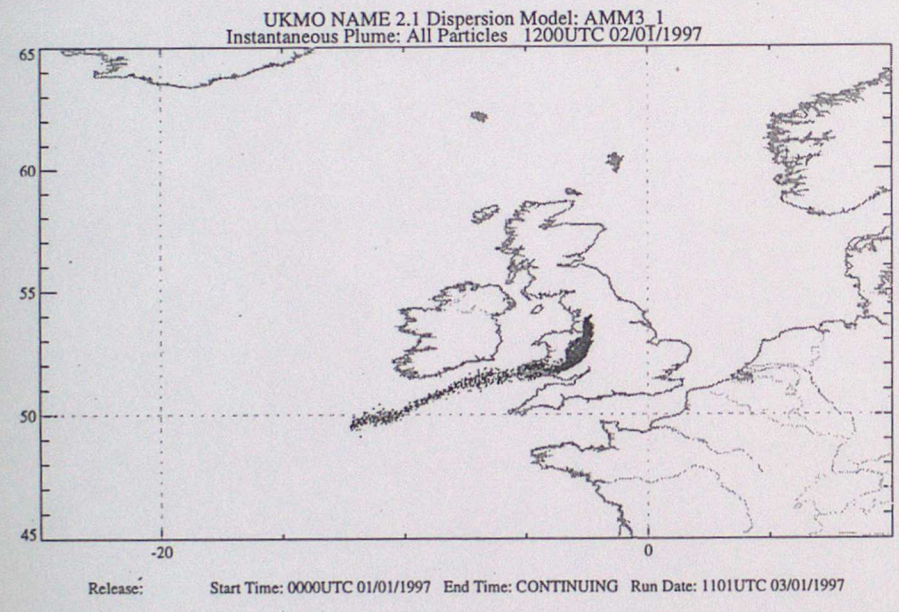

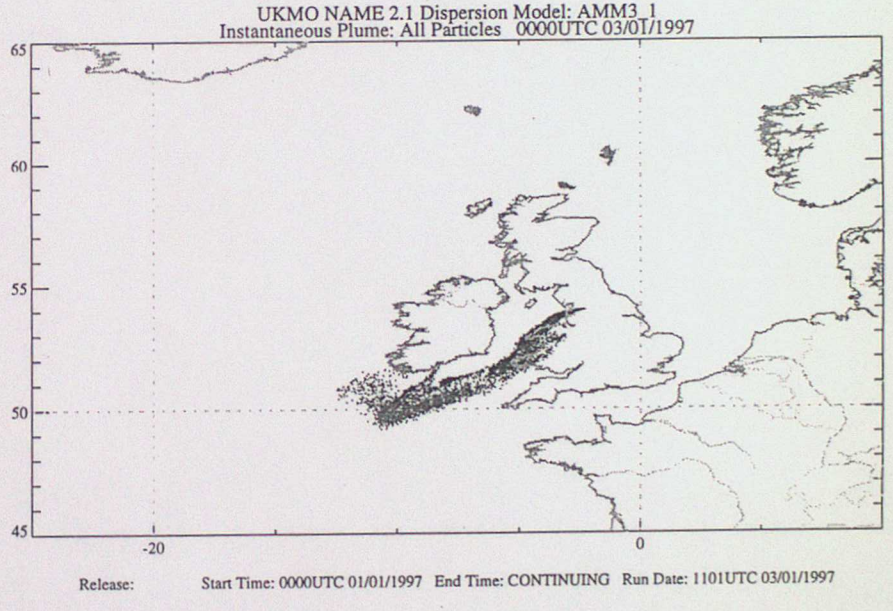

Fig. 6c *Mesoscale Input*

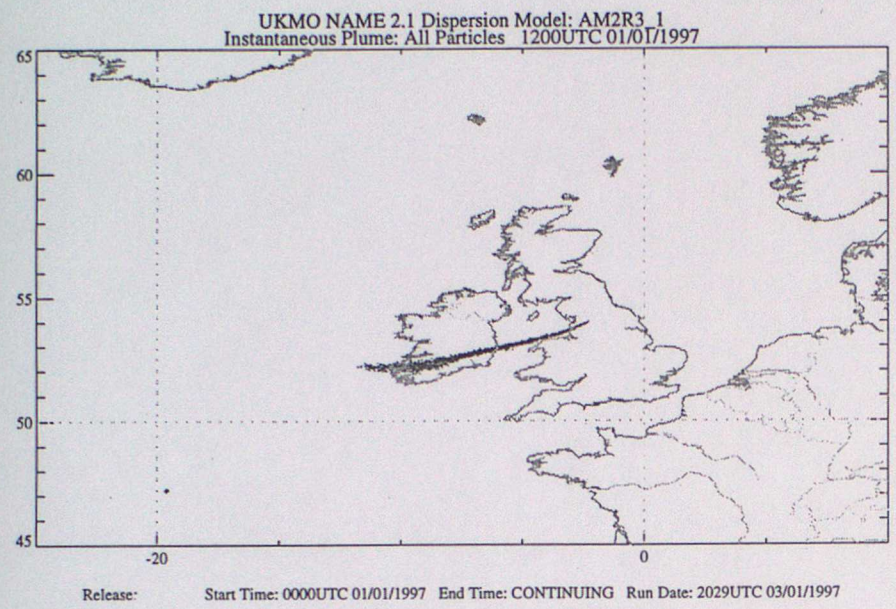

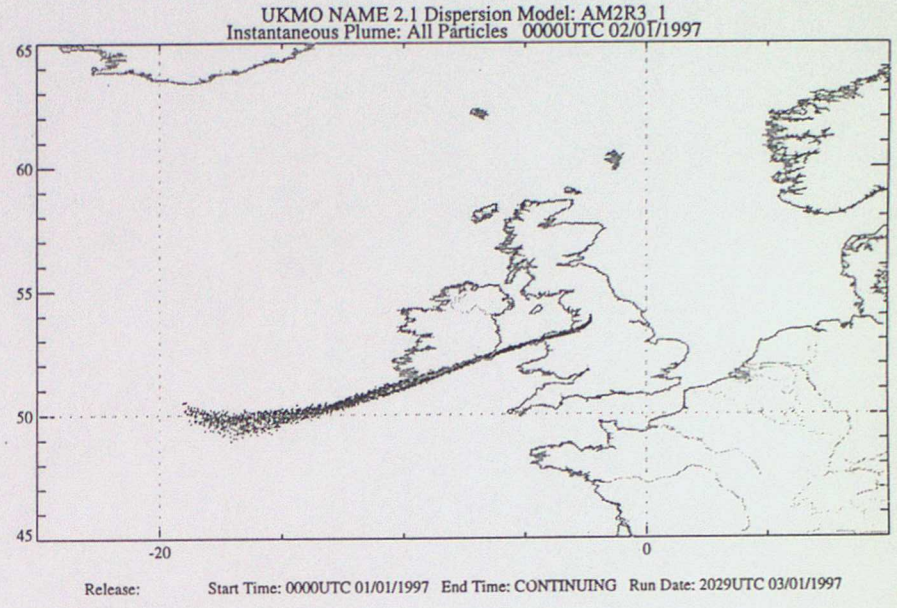

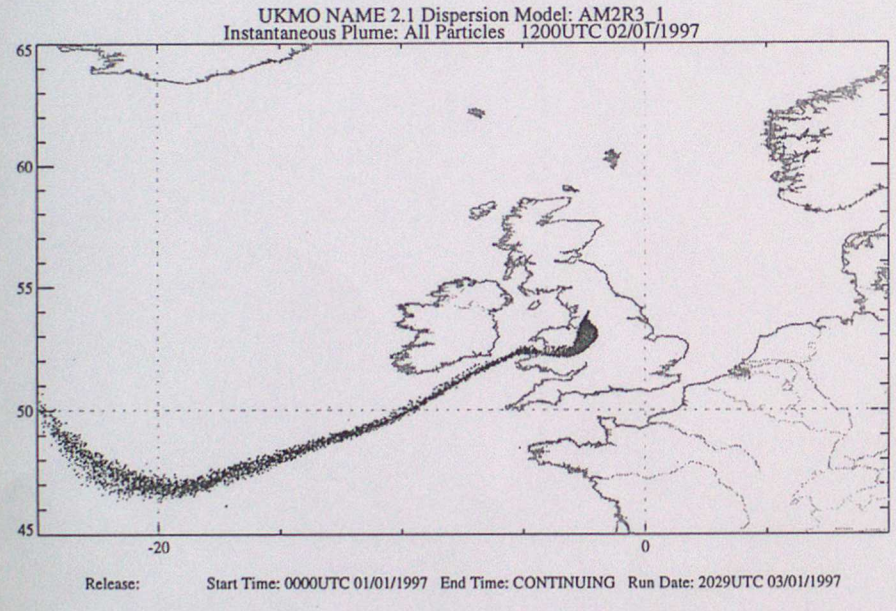

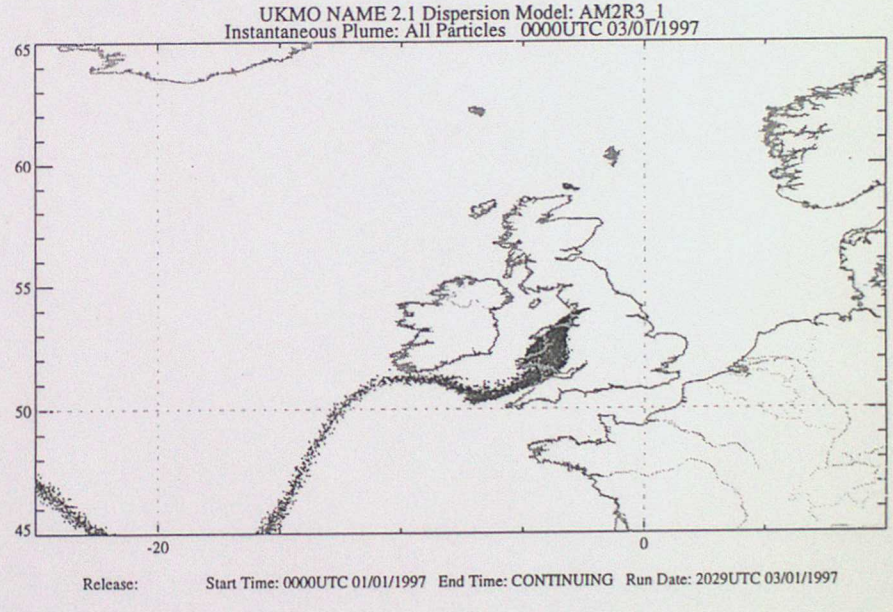

Fig 6d. *Regional Input - no meander*

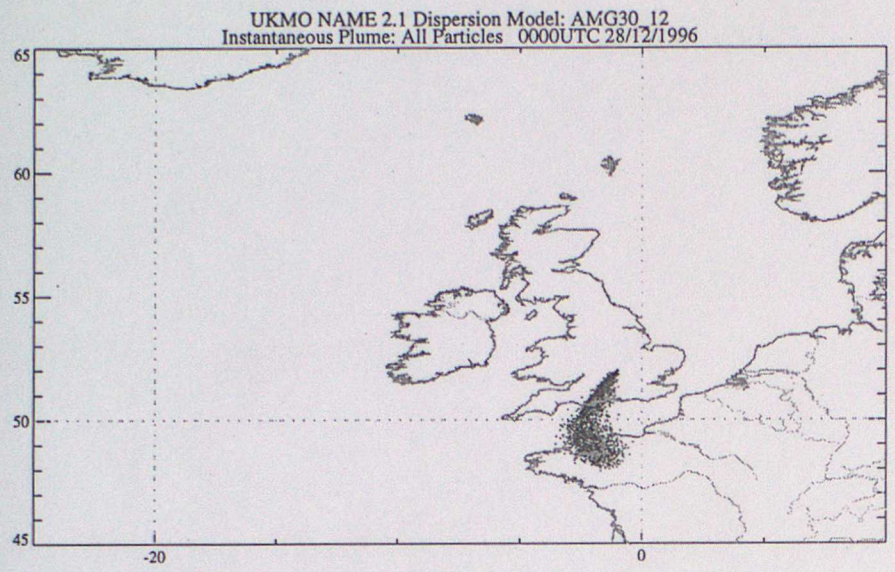

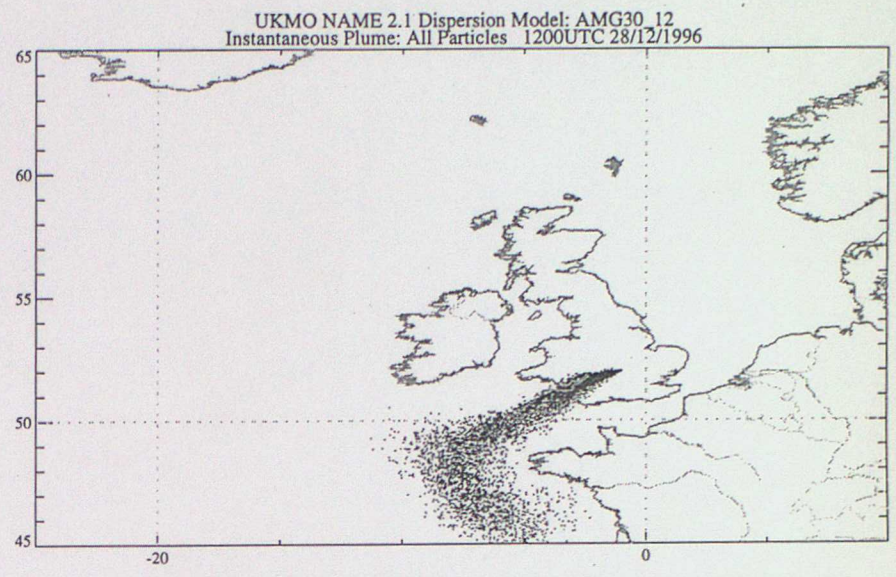

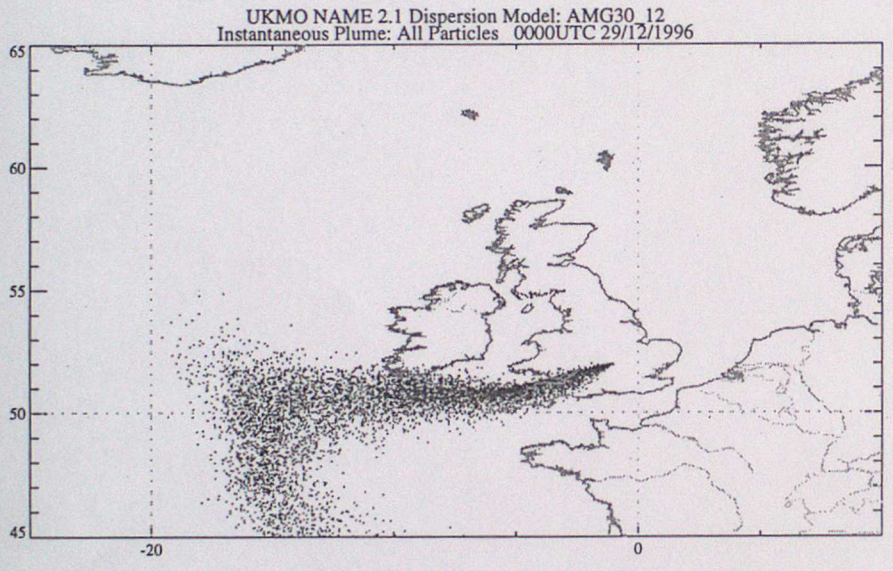

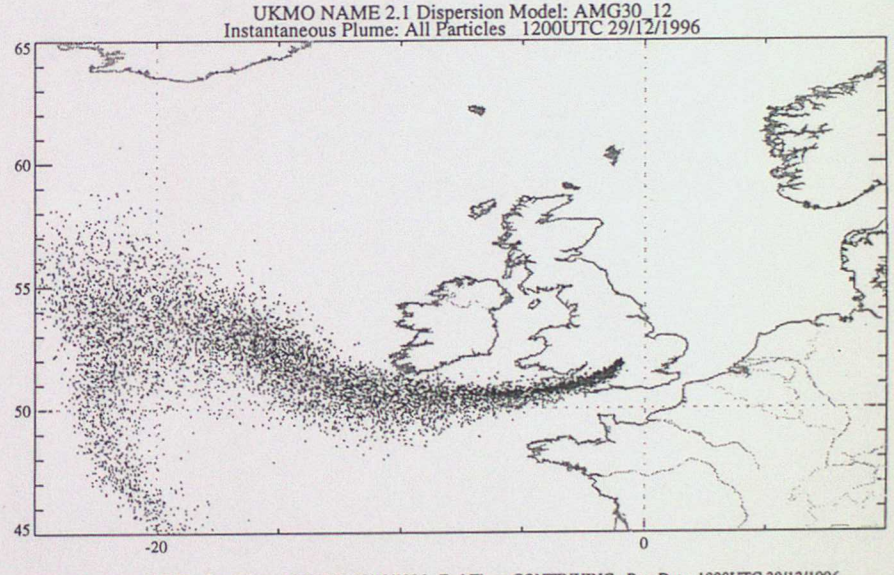

Fig 7a *Global Input*

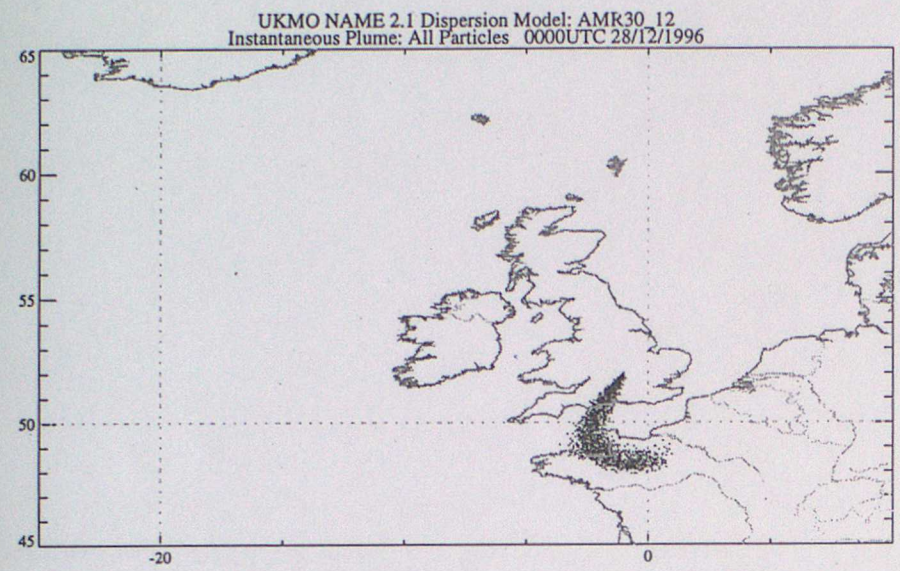

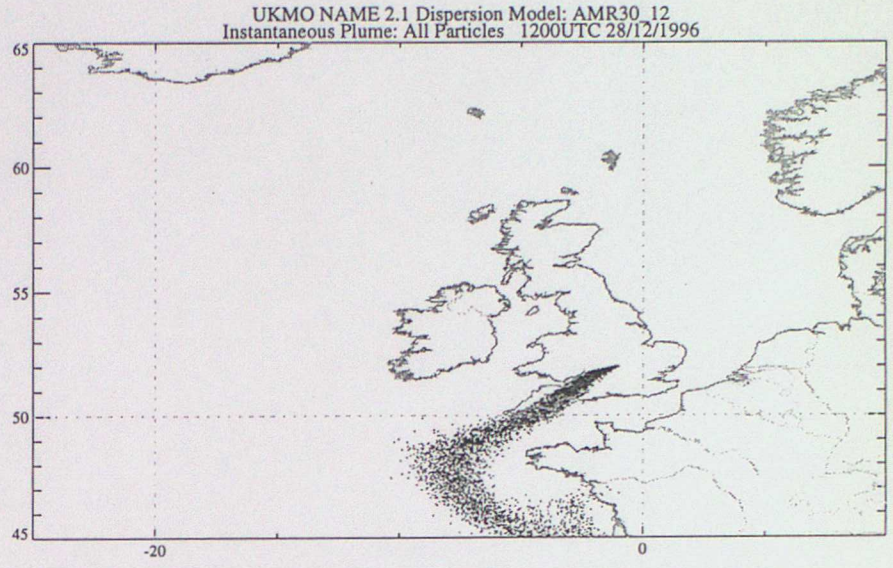

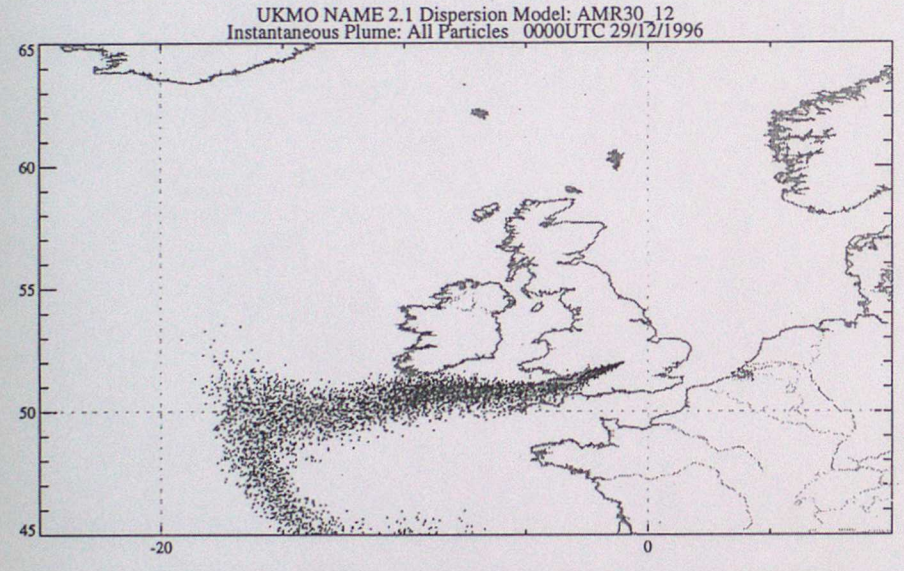

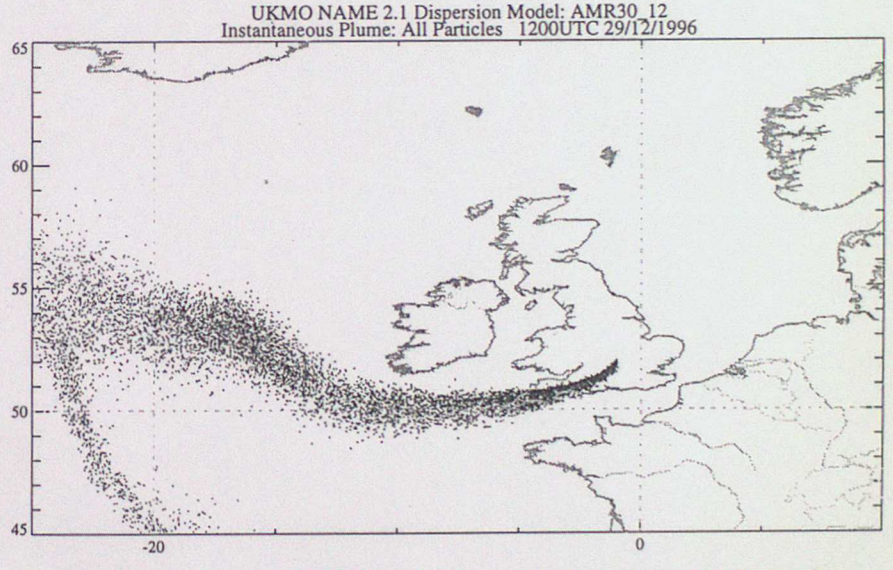

Fig 7b *Regional Input*

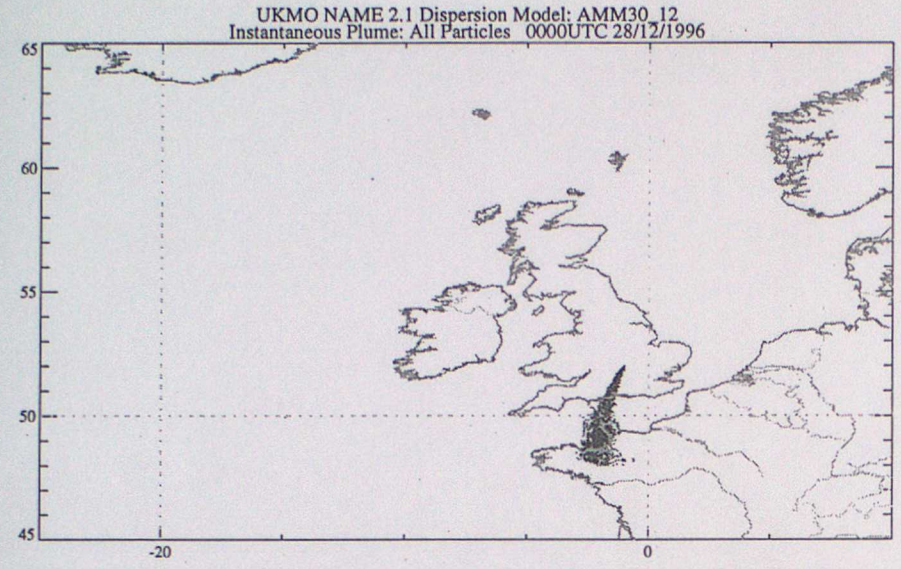

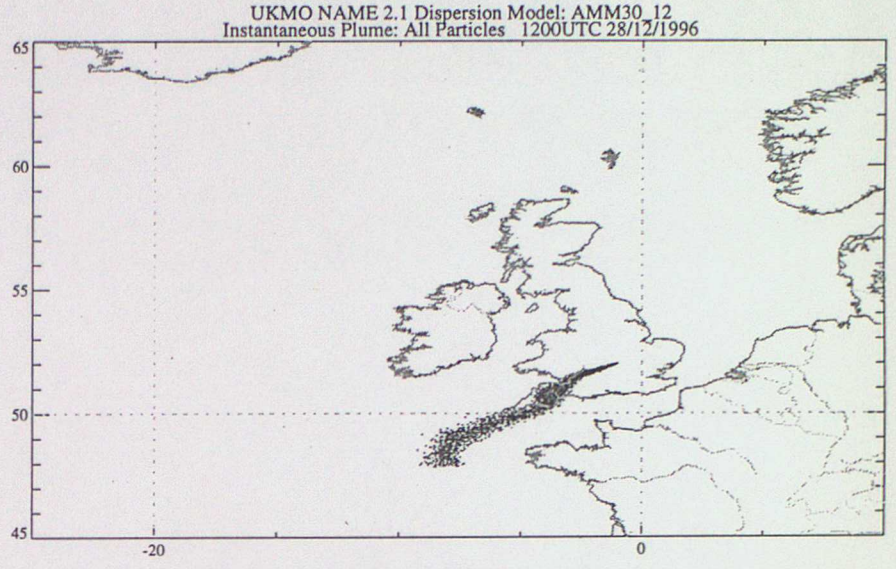

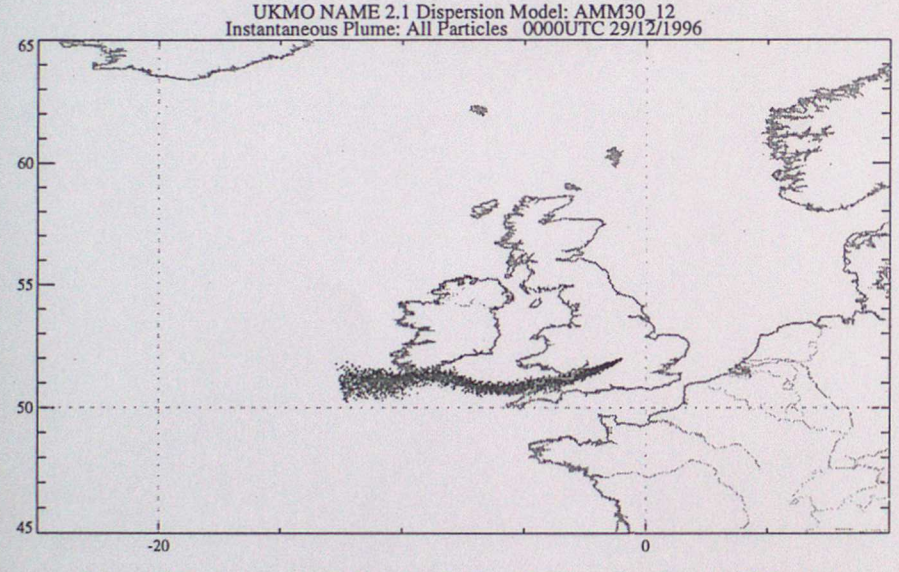

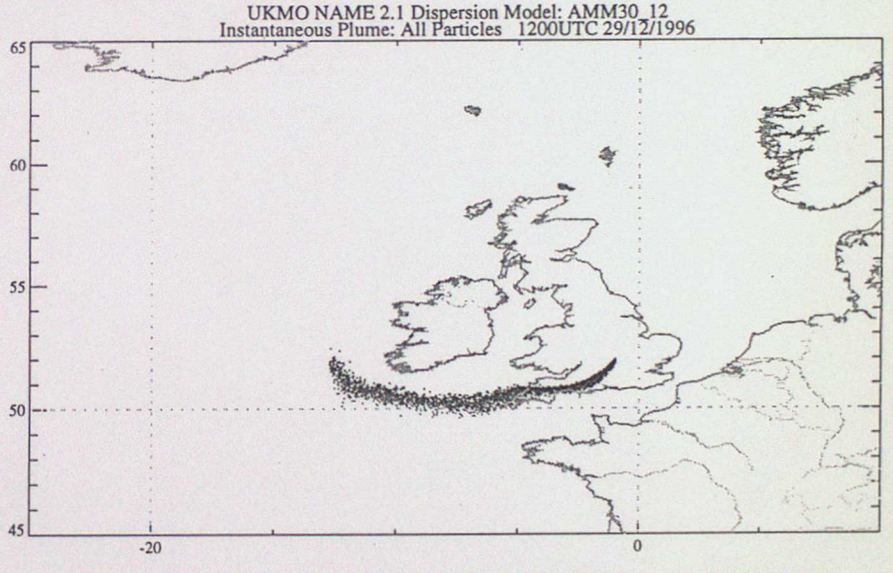

Fig 7c *Mesoscale Input*